Supporting Information Appendix for

KidA, a multi-PAS domain protein, tunes the period of the cyanobacterial circadian oscillator

Soo Ji Kim, Chris Chi, Gopal Pattanayak, Aaron R. Dinner, and Michael J. Rust

Supplementary Materials and Methods

Cyanobacterial strain construction

For overexpression strains, the gene of interest was integrated into the Neutral Site 1 (NS1) of the *S. elongatus* genome. The coding sequence of the gene of interest + C-terminal HA tag (TACCCATACGATGTTCCAGATTACGCT) was inserted into pAM2991 plasmid downstream of the IPTG-inducible pTrc promoter and upstream of the spectinomycin resistance gene cassette, which are flanked by the NS1 sequences (1). Strains constructed this way include the KaiB$^{G88A;D90R}$-HA (fsKaiB-HA) strain used in the co-IP/MS experiment, KidA-OX, and KidA domain truncation mutant overexpression strains. Wild type *S. elongatus* was used as the background for fsKaiB-HA. WT/pAM2195 reporter strain (MRC1005), which carries PpsbAI :: luxAB, PpsbAI :: luxCDE at NS 2.1, was used as the background for KidA-OX and KidA domain truncation mutant overexpression strains (2, 3). For the KidA knockout strain (Δ*kidA*), two ~500 bp long stretches of *S. elongatus* genome sequence directly upstream and downstream of *kidA* coding sequence were inserted into the pMR0089 plasmid to flank the gentamicin resistance cassette. By homologous recombination, the native KidA gene in WT/pAM2195 strain was replaced with the gentamicin resistance gene. After propagation on selective media, all mutant alleles were verified by PCR to have fully segregated. The plasmids and strains used in this study are outlined in Supplementary Information Table 1.

Anti-HA co-IP from cyanobacterial lysate

Cyanobacterial cells were harvested at OD750 = 0.7–1 by centrifugation at 25 °C at maximum speed and were stored in -80 °C after being snap-frozen in liquid nitrogen. Cells from ~45 ml of culture were used per co-IP experiment. Cells were thawed, pelleted, and resuspended in 250 µl of lysis buffer composed of 50 mM HEPES (pH 7.5), 1 mM EDTA, 1 mM DTT, 0.2% Triton X-100, 50mM NaCl, protease inhibitor, and phosphatase inhibitor. After a 20-minute incubation at 4 °C with gentle agitation, ~100 µl of 0.1 mm glass beads were added, followed by bead beating (10 reps of 30 seconds vortexing and 30 seconds to 1 minute cooling on ice). The lysed mixture was clarified by centrifugation for 3 minutes at 10000 g. The resulting supernatant was transferred to a new tube and further centrifugated for 1 hour at 9000 g at 4 °C. 50 µl of the supernatant from this second spin was saved as input, and the rest was mixed with Anti-HA magnetic beads (MBL Catalog # M132-11) that were isolated from 50 µl resuspended slurry and equilibrated with the same lysis buffer. The mixture was incubated at 4 °C for 30 minutes with gentle agitation. The beads were pelleted by magnet and the supernatant was removed. After washing with the lysis buffer three times, the samples were eluted by incubating the beads in 60 µl of 0.1 M Glycine (pH 2) for 10 minutes at room temperature. The beads were removed from the eluate by magnet, and the eluate was neutralized by the addition of ~12 µl of 1 M Tris (pH 8).

LC-MS/MS analysis of fsKaiB co-IP samples

The eluate samples from the co-IP were submitted to the Harvard Center for Mass Spectrometry (Cambridge, MA) for LC-MS/MS analysis. The samples were first treated using 20mM TCEP/50mM TEAB (Sigma) (1/10 vol/vol ratio, 37 °C incubation for 1 hour, cooled to room temperature for 10 minutes, followed by vortex and spin). Next, 40 mM iodoacetamide (Sigma)/50mM TEAB was added to the sample (1/10 vol/vol ratio, 1 hour incubation at room temperature under tin foil), followed by a 16-hour, 37 °C incubation with Trypsin (Promega) in thermo mixer. The digested samples were vortexed and transferred to an HPLC and was dried to 30 µl to shoot 14/30 µl on Mass Spec. LC-MS/MS was performed on a Orbitrap Elite Hybrid Ion Trap-Orbitrap Mass

Spectrometer (Thermo Fischer, San Jose, CA) equipped with WATERS Acquity nano pump nanoLC (WATERS Corp. Milford, MA). Peptides were separated onto a 100 µm inner diameter microcapillary trapping column packed first with approximately 5 cm of C18 Reprosil resin (5 µm, 100 Å, Dr. Maisch GmbH, Germany) followed by WATERS analytical column. Separation was achieved through applying a gradient from 5–27% ACN in 0.1% formic acid over 90 min at 200 nl min^{-1}. Electrospray ionization was enabled through applying a voltage of 1.8 kV using a home-made electrode junction at the end of the microcapillary column. The Elite Orbitrap Velos was operated in data-dependent mode for the mass spectrometry methods. The mass spectrometry survey scan was performed in the Orbitrap in the range of 395–1,800 m/z at a resolution of 6 × 104, followed by the selection of the thirty most intense ions (TOP30) for CID-MS2 fragmentation in the Ion trap using a precursor isolation width window of 2 m/z, AGC setting of 10,000, and a maximum ion accumulation of 200 ms. Singly charged ion species were not subjected to CID fragmentation.

For the analysis, raw data were submitted in Proteome Discoverer 2.3 software (Thermo Scientific). Assignment of MS/MS spectra was performed using the Sequest HT algorithm by searching the data against a protein sequence database including all entries from the center's Uniprot_Synechococcus ElongatusPCC7942.fasta database as well as other known contaminants such as human keratins and common lab contaminants. Sequest HT searches were performed using a 20-ppm precursor ion tolerance and requiring each peptides N-/C termini to adhere with Trypsin protease specificity, while allowing up to two missed cleavages. A MS2 spectra assignment false discovery rate (FDR) of 1% on both protein and peptide level was achieved by applying the target-decoy database search. Filtering was performed using a Percolator (64bit version) (4). Peptide N termini and lysine residues (+229.162932 Da) was set as static modifications while methionine oxidation (+15.99492 Da) was set as variable modification.

Anti-HA Western blot

For the experiment shown in Supplementary Figure S2A, 75 ml of KidA-OX strain was grown in 30 °C shaker under constant light to the OD_{750} of ~ 0.6, which was divided into four 5 ml cultures in glass tubes. At this point, 0, 10, 30, or 70 µM IPTG was added to each culture, which was induced for 20.5 hours in 30 °C with shaking. 4 ml of culture was pelleted and flash frozen in liquid nitrogen. The pellets were resuspended in lysis buffer (8 M Urea, 20 mM HEPES pH 8, 1 mM $MgCl_2$) and lysed using bead beating as described above. Same amounts of lysate, adjusted based on the total protein levels measured by Bradford assay, were subjected to an SDS-PAGE electrophoresis using a 4-20% Criterion TGX gel (Bio-Rad). Proteins separated in the gel were transferred to PVDF membrane via wet transfer. The membrane was blotted using Anti-HA antibody (Biolegend Catalog # 901501) followed by HRP-conjugated secondary antibodies. The membranes were processed with SuperSignal West Femto kit (Thermo Scientific) and visualized using ChemiDoc (Bio-Rad).

***In vivo* clock rhythm measurement**

A black 96-well plate (Costar) was prepared by filling each well with 250 µl of a BG11M + 0.9% Gelzan (Sigma) pad mixture in off-the-boil liquid state, which then solidified at room temperature. For experiments involving IPTG induction, 10 µl of IPTG solution was added on top of the media pad. The concentration of the IPTG solution was chosen so that the equilibrium concentration in the pad matched the target concentration. E.g., a 0.25 mM IPTG solution was used for 10 µM IPTG induction, which was chosen as the default condition for characterizing clock phenotypes of KidA overexpression strain (condition used for Figures 2A, 2B, 2D, and 2E). At least 3 hours after IPTG addition, 30 µl of cells at OD_{750} of 0.1–0.3 were added on top of the media pad. The plate was sealed with a transparent film (UniSeal, GE HealthCare Life Sciences) with holes punched by a 26G½ needle (BD, Franklin Lakes, NJ, Cataloog # 305111) above each well. The plate was placed under a red LED array described in (5) that was programmed to turn on and off accordingly during the entrainment or dark pulse applications, and to stay on for constant light. Every 30 minutes after the initiation of the LED light program, bioluminescence from each well was measured using a TopCount plate reader (PerkinElmer).

Circadian rhythm data fitting and phase response curve analysis

All experimental circadian rhythm data were fit to the following equation:

$$Y = \text{Offset} + \text{Slope} \cdot X + \text{Amplitude} \cdot \sin\left(\frac{2\pi(X - \text{PhaseShift})}{\text{Period}}\right)$$

Oscillatory traces from individual samples were fit separately, and the best-fit values for each parameter were averaged across replicates. GraphPad Prism was used for data shown in Figure 3D, 4A, and 4D, and a custom-written Matlab code optimized for generating initial guesses for the parameters was used for analyses in Figures 2C, 2D, and 2E. A time-window greater than 48 h was used to fit each data set. We excluded the initial transient in the data when cultures are rapidly growing (typically the first 12 h). For KidA-OX in Figure 2C, only data up to 60 hours in constant light were used to fit the period, because of the arrhythmicity outside of this window in >30 μM IPTG conditions (Supplementary Figure S2). To produce the phase response curves in Figure 2E, we first aligned the data for each strain and each condition by shifting the time axis to place the trough of the constant light reporter rhythm prior to the dark pulse at CT = 0. We then rescaled the time axis by a factor 24 h / (FRP), where FRP is the free-running period for strain, estimated by the fitting procedure described above.

Tertiary structure prediction by Phyre2

The Phyre2 algorithm (6) was used to predict local structures in KidA's N-terminal region for domain prediction reported in Figure 3B. The N-terminal region was divided into two parts, a domain predicted to be a PAS domain due to high sequence homology (residues 360 to 485, corresponding to PAS-D) and the rest (residues 1 to 359). The outputted 3D structure files from the two submissions were visualized by VMD (7) and for each of the four local tertiary structures, the secondary structure information of each residue was mapped. Intensive mode was used for residues 1 to 359, which resulted in 351 residues (98%) modelled at >90% accuracy. Normal mode was used for residues 360 to 485, which resulted in 99.9% confidence in the model.

***In vitro* co-IP using FLAG-tagged proteins as bait**

Each co-IP sample (20 μl) was prepared in Kai reaction buffer (10% glycerol, 20 mM Tris-HCl pH 8, 150 mM NaCl, 5 mM $MgCl_2$, 0.5 mM EDTA pH 8, 1 mM ATP pH 8) and snap-frozen in liquid nitrogen at the end of desired length of co-incubation. (*See below for details of sample preparation for each experiment.*) To isolate the bait protein and its interactors, Anti-FLAG M2 Magnetic beads (Sigma-Aldrich) were used. 10 μl of resuspended bead slurry was used for each co-IP reaction. Beads were washed with Kai reaction buffer by two cycles of pelleting on magnet, buffer removal, and resuspension, and then were resuspended with 10 μl of the reaction sample for binding reaction. After incubating for 10 minutes at 22 °C while shaking at 950 rpm, beads were pelleted on magnet. The supernatant was removed, and the beads were washed twice using Kai reaction buffer. Proteins bound to the beads were then eluted by incubation in 10 μl of 0.75 mg/ml 3x FLAG peptide (Sigma-Aldrich) solution for 40 minutes at 22 °C with 950 rpm shaking. The final supernatant after pelleting the beads was transferred into a fresh tube and centrifugated for 1 minute for complete exclusion of the beads. 7.5 μl of the supernatant was saved and stored in -20 °C. The co-IP samples were visualized by performing SDS-PAGE electrophoresis using precast 4-20% Criterion TGX gel (Bio-Rad), staining the gel using Sypro Ruby (Invitrogen), and imaging the gel using ChemiDoc (Bio-Rad). The band intensity was quantified using ImageJ software by manually defining the rectangular area of each band, along with the background intensity from the neighboring area that was deducted from the band intensity.

Sample preparation for co-IP:

For all co-incubation of purified proteins in this study, samples were incubated in 30 °C. For the experiment shown in Figure 3E and Supplementary Figure S4, 3.5 μM of wtKaiB-FLAG or fsKaiB-FLAG (KaiB-1-99-Y7A-I87A-Y93A-FLAG) was mixed with 3.5 μM of KidA PAS-ABC or KaiC-EA in Kai reaction buffer. The mixture was incubated for 30 minutes or 20 hours. For the experiment in Figure 3F, 3.5 μM wtKaiB-FLAG was pre-incubated with 0, 0.7, or 3.5 μM of KidA PAS-ABC for 1, 5, or 20 hours. For the experiment in Supplementary Figure S5, the following concentrations were used for each protein: 3.5 μM KaiB-FLAG, 3.5 μM KaiC-EA, 1.5 μM KaiA, and 3.5 μM KidA PAS-ABC. At the end of intended duration of co-incubation, the samples were snap-frozen in liquid nitrogen and stored at -20 °C. After the samples were thawed, they were immediately subjected to the co-IP procedure, except for the experiment in Figure 3F where 3.5 μM KaiC-EA was added to the thawed reaction and incubated at 30 °C for 5 minutes prior to co-IP.

Fluorescence Polarization

Clock reactions were prepared by mixing Kai proteins at their standard concentrations (1.5 μM KaiA, 3.5 μM KaiB, 3.5 μM KaiC) along with 0.2 μM FITC-labeled $KaiB^{K25C}$ in the clock reaction buffer containing 1 mM ATP, similar to the procedure used previously (5). KidA PAS-ABC was added to the reaction at specified concentrations. 30 μl of the reaction mixture was added to a black 384-well plate, which was sealed with non-fluorescent film (Thermo Scientific, #232698). The plate was loaded into a plate reader (Tecan), which was used to measure fluorescence polarization with 485 nm excitation (20 nm bandpass) and 535 nm emission (25 nm bandpass) using a 510nm dichroic filter. Measurements were taken every 15 min. Reaction buffer-only wells were used as blank.

KaiA-induced KaiC phosphorylation and KaiC auto-dephosphorylation

For KaiA-induced KaiC phosphorylation with or without KidA PAS-ABC, KaiC was first dephosphorylated by incubation at 30 °C for 27 hours. The master mix for each reaction was prepared as follows: 0.4 μM KaiA + 3.5 μM KaiC (negative control), 0.4 μM KaiA + 3.5 μM KaiC + 1.5 μM KidA PAS-ABC (low KidA condition), 0.4 μM KaiA + 3.5 μM KaiC + 3.5 μM KidA PAS-ABC (high KidA condition) in the Kai reaction buffer. KaiA was added last. The master mix reaction was divided into 20 μl aliquots, which were incubated in 30°C. One aliquot of each reaction condition was quenched every 30 minutes by adding 3x SDS-PAGE loading buffer to the sample and was stored in -20 °C. The samples for t = 0 were harvested by having the 3X SDS-PAGE loading buffer pre-loaded in the tubes before aliquoting. KaiC auto-dephosphorylation sampling was done in a similar manner, except the KaiC aliquot that was taken out from the –80 °C was used immediately after thawing and no KaiA was added. For both experiments, KaiC phosphoform composition at each timepoint was resolved by SDS-PAGE analysis using 10% acrylamide gel (37.5:1 acrylamide:bis-acrylamide), run for 4.5 hours under 30 mA constant current at 12 °C. The gel was stained by SimplyBlue SafeStain (Invitrogen) and imaged using Odyssey imager (LI-COR) or ChemiDoc (Bio-Rad).

Modeling Background

Here, we provide a brief description of the original model of Paijmans *et al*. (8), which we henceforth term the Paijmans model.

The fundamental unit in the Paijmans model is a KaiC hexamer, and exchange of subunits between hexamers is not considered. The CI domain has a nucleotide binding site that can hydrolyze ATP, a KaiB binding site, and (via associated KaiB) an inhibitory KaiA binding site; the CII domain of each subunit has a nucleotide binding site that can transfer phosphoryl groups to and from S431 and T432 and hydrolyze ATP, and there is a single shared KaiA binding site that acts on all the CII domains in a hexamer. ATP and ADP are assumed to be in excess, such that the nucleotide binding sites are always occupied. CII domains exchange nucleotides only when KaiA is bound to the shared site, with rates that are proportional to the solution concentration of the alternate nucleotide form; CI domains exchange ADP for ATP at a constant rate and become occupied by ADP only through hydrolysis. In the original Paijmans model, the solution concentration of fsKaiB is assumed to be constant, such that binding of KaiB to the CI domain occurs with kinetics that are first-order in the concentration of available CI sites.

In analogy to the Monod-Wyman-Changeux model of cooperativity, a KaiC hexamer can exist in two states, termed active and inactive. The free energy of the inactive state decreases relative to that of the active state proportionally to the number of phosphorylated serines in the CII domain, ADPs bound in the CI domain, KaiB molecules bound to the CI domain, and KaiA dimers bound to the CI domain. When in the inactive state, the CI domain has a higher affinity for KaiB, and with six KaiB monomers bound, the CI domain can sequester up to six KaiA dimers.

Enumerating all the possible combinations of states of each of the sites for a KaiC hexamer results in an intractably large number of ordinary differential equations, and instead trajectories of the model are generated by kinetic Monte Carlo simulations, which sample only a small fraction of the combinations. Parameters are

selected such that the model is thermodynamically consistent: detailed balance (microscopic reversibility) is enforced for all reactions that do not involve ATP hydrolysis.

Modeling KidA

To test the hypothesis that KidA shortens the period of the oscillator by selectively binding to and stabilizing fsKaiB, we modified the Paijmans model to treat KaiB explicitly as follows.

KaiB fold switching is modeled on the monomer level. The KaiB tetramer is not considered. Individual KaiB monomers interconvert between ground state (gs) and fold switched (fs) forms:

$$\mathrm{KaiB_{gs}} \underset{\mathrm{kBswitch_r}}{\overset{\mathrm{kBswitch_f}}{\rightleftharpoons}} \mathrm{KaiB_{fs}}$$

KidA only binds fsKaiB, and any KaiB in complex with KidA cannot convert to the ground state until after dissociation:

$$\mathrm{KidA} + \mathrm{KaiB_{fs}} \underset{\mathrm{kKidA_{off}}}{\overset{\mathrm{kKidA_{on}}}{\rightleftharpoons}} \mathrm{KidA \cdot KaiB_{fs}}$$

Each of the KaiB species can bind to the CI domain with second-order kinetics. fsKaiB and KaiB·KidA complexes bind to CI at the same rate. KaiB in complex with CI is assumed to always be in the fold-switched state, but if not also bound to KidA, KaiB can dissociate from CI directly to the ground state (and the reverse reaction consisting of simultaneous gsKaiB binding and transition to the fold-switched form is included for detailed balance). Different rates are used for active and inactive CI (denoted by $\mathrm{i} \in \{\mathrm{A}, \mathrm{I}\}$ below):

$$\mathrm{CI_i} + \mathrm{KaiB_{fs}} \underset{\mathrm{kCI_iB_{fs,off}}}{\overset{\mathrm{kCI_iB_{fs,on}}}{\rightleftharpoons}} \mathrm{CI_i \cdot KaiB}$$

$$\mathrm{CI_i} + \mathrm{KidA \cdot KaiB_{fs}} \underset{\mathrm{kCI_iB_{fs,off}}}{\overset{\mathrm{kCI_iB_{fs,on}}}{\rightleftharpoons}} \mathrm{CI_i \cdot KidA \cdot KaiB}$$

$$\mathrm{CI_i} + \mathrm{KaiB_{gs}} \underset{\mathrm{kCI_iB_{gs,off}}}{\overset{\mathrm{kCI_iB_{gs,on}}}{\rightleftharpoons}} \mathrm{CI_i \cdot KaiB}$$

$$\mathrm{KidA} + \mathrm{CI_i \cdot KaiB} \underset{\mathrm{kKidA_{off}}}{\overset{\mathrm{kKidA_{on}}}{\rightleftharpoons}} \mathrm{CI_i \cdot KidA \cdot KaiB}$$

KidA does not interfere with KaiA binding to CI·KaiB complexes, so the reactions of the original model are sufficient to treat KaiA binding.

As in the original Paijmans model, detailed balance is enforced for each reversible reaction. This allows for the constraints

$$\mathrm{kCI_iB_{g,off}} = \frac{\mathrm{kCI_iBG_{on}}\ \mathrm{kCI_iB_{fs,off}}\ \mathrm{kBswitch_r}}{\mathrm{kBswitch_f}\ \mathrm{kCI_iB_{fs,on}}}$$

where $\mathrm{i} \in \{\mathrm{A}, \mathrm{I}\}$, with i representing the same state in all rate constants within an equation (i.e., there are two such constraint equations in total, one for the active state rate constants and one for the inactive state rate constants).

Parameter exploration

We used Markov Chain Monte Carlo (MCMC) sampling to explore the values of the parameters that we added to extend the model while keeping the parameters of the original Paijmans model at their published values. Specifically, we employed the Goodman-Weare affine invariant sampling scheme, in which an ensemble of parameter sets is simulated in parallel and used to guide the directions of MC moves (9). During sampling, we represented the parameter values by their natural logarithms; this guaranteed that the rate constants remained positive.

We used an ensemble size of 50 and walk moves with the move size parameter set to 1. For each parameter set, we performed two simulations. Both simulations were 430 hours long with 1.2 μM KaiA dimers, 1.2 μM KaiC hexamers, and 4.8 μM KaiB monomers. One simulation was performed with 0 μM KidA, and the other was performed with 0.7 μM KidA. Initial ensemble members were generated by drawing their parameter values uniformly from ranges of 2×10^{-4} centered on the natural logarithms of the initial values listed in SI Table 4. To set the initial values of the KaiB binding rates, we determined the concentration of fsKaiB for the isolated fold switching equilibrium (i.e., $[\mathrm{fsKaiB}]_{\mathrm{iso}} = [\mathrm{KaiB}]_0/(1 + \mathrm{kBswitch_r}/\mathrm{kBswitch_f})$) and then set $\mathrm{kICIB_{fs,on}}$ and $\mathrm{kACIB_{fs,on}}$ such that $\mathrm{kICIB_{fs,on}}[\mathrm{fsKaiB}]_{\mathrm{iso}}$ and $\mathrm{kACIB_{fs,on}}[\mathrm{fsKaiB}]_{\mathrm{iso}}$ were equal to the corresponding first-order rates in the original Paijmans model. The initial KaiB unbinding rates were set to be the same as those in the original Paijmans model. Other parameters were chosen in an ad hoc fashion to reproduce experimental observations qualitatively. Two independent MCMC sampling runs for 200 sweeps over the ensemble were performed with different constraints; the acceptance rate was 40% in both cases.

For both sampling runs, proposed parameter sets that produced nonoscillatory trajectories were rejected. Parameter sets that supported oscillations at both 0 μM KidA and 0.7 μM KidA were subject to the following additional biases. To favor trajectories with periods close to 24 hours in the absence of KidA, the squared difference between the period of a trajectory and 24 hours was subtracted from the log likelihood. To ensure that KaiB binds faster to inactive KaiC than it does to active KaiC, if any KaiB binding rate to active KaiC is greater than the corresponding binding rate to inactive KaiC, the squared difference between logarithms of the two binding rates was subtracted from the log likelihood. Similarly, to ensure that fsKaiB binds to KaiC faster than gsKaiB does, if the difference between the natural logarithm of any fsKaiB binding rate and the natural logarithm of the corresponding gsKaiB binding rate is less than nine (i.e., 10^4 fold), the squared difference between nine and the aforementioned difference between the log rates is subtracted from the log likelihood. These contributions to the log likelihood are

$$\begin{aligned} L_0 = (-(T_0 - 24)^2 &- \mathbf{1}\{\ln(\mathrm{kCI_AB_{fs,on}}) - \ln(\mathrm{kCI_AB_{gs,on}}) < 9\}(9 - \ln(\mathrm{kCI_AB_{fs,on}}) + \ln(\mathrm{kCI_AB_{gs,on}}))^2 \\ &- \mathbf{1}\{\ln(\mathrm{kCI_IB_{fs,on}}) - \ln(\mathrm{kCI_IB_{gs,on}}) < 9\}(9 - \ln(\mathrm{kCI_IB_{fs,on}}) + \ln(\mathrm{kCI_IB_{gs,on}}))^2 \\ &- \mathbf{1}\{\ln(\mathrm{kCI_AB_{fs,on}}) > \ln(\mathrm{kCI_IB_{fs,on}})\}(\ln(\mathrm{kCI_AB_{fs,on}}) - \ln(\mathrm{kCI_IB_{fs,on}}))^2 \end{aligned}$$

In the equation above, T_0 is the period at 0 μM KidA and $\mathbf{1}\{\cdot\}$ is an indicator function equal to one if the condition is satisfied and zero otherwise. The biases on the binding rates to active and inactive KaiC are imposed to preserve the roles of those species in the original Paijmans model. The biases on the binding rates of gsKaiB and fsKaiB are imposed so that the effect of KidA on KaiB binding to KaiC is not overwhelmed by the baseline level of KaiB binding: as the gsKaiB binding rate increases, the increased solution concentration of fsKaiB has less impact. Additionally, if the gsKaiB binding rates are greater than the fsKaiB binding rates, the roles of gsKaiB and fsKaiB invert, making the model inconsistent with the established behavior of KaiB.

In the first sampling run, to encourage the sampling of biochemically reasonable values of the affinity of KidA for fsKaiB, a penalty equal to the square of the difference between –7.4 and the natural logarithm of the K_d in units of μm^{-3} of the KidA-fsKaiB binding interaction was subtracted from the log likelihood whenever this quantity was less than –7.4 (corresponding to K_d values smaller than 10^{-11} M). A similar penalty was also subtracted from the log likelihood when the natural logarithm of the K_d in units of μm^{-3} was greater than 6.4 (corresponding to K_d values greater than 10^{-5} M). The total log likelihood for oscillatory trajectories was then

$$\begin{aligned} L_1 = L_0 &- \mathbf{1}\{\ln(\mathrm{kKidA_{off}}) - \ln(\mathrm{kKidA_{on}}) < -7.4\}(\ln(\mathrm{kKidA_{off}}) - \ln(\mathrm{kKidA_{on}}) + 7.4)^2 \\ &- \mathbf{1}\{\ln(\mathrm{kKidA_{off}}) - \ln(\mathrm{kKidA_{on}}) > \ \ 6.4\}(\ln(\mathrm{kKidA_{off}}) - \ln(\mathrm{kKidA_{on}}) - 6.4)^2 \end{aligned}$$

In the second sampling run, the constraints on the K_d of the KidA-KaiB binding interaction were replaced with a penalty subtracted from the log likelihood equal to the squared difference between the period with 0.7 μM KidA and 20 hours (to constrain the slope to be –5.7 hours / μM KidA), giving a total log likelihood of

$$L_2 = L_0 - (T_{0.7} - 20)^2$$

where $T_{0.7}$ is the period in hours at 0.7 μM KidA.

We show the distributions of period and amplitude sensitivities to [KidA], as represented by the slopes in Figure 4D, in Figure S7. To estimate the periods, we computed the autocorrelation function of the average number of KaiB bound per KaiC hexamer and then averaged the times between peaks in the autocorrelation function. To determine peak times, the autocorrelation function was interpolated using quadratic splines near each peak. We estimated the amplitudes as the average peak prominence, normalized to 1 for 0 μM KidA. Because the period and amplitude as functions of KidA concentration were generally well fit by lines, we estimated the slopes for Figures S7 and S8 from only the periods and amplitudes of the oscillator with 0 μM KidA and 0.7 μM KidA. The parameter set used to generate Figure 4 was selected from the MCMC results obtained with log likelihood L_1 to have period and amplitude slopes closest to the experimentally observed ones, while maintaining a near-24-hour period in the absence of KidA. The parameter values used to generate Figure 4 are listed in SI Table 4.

To determine which parameters contributed the most to the period slope, the nonparametric Spearman correlation coefficient was computed pairwise between all parameters, the period and amplitude slopes, and the dissociation constant of the KidA-fsKaiB binding interaction (KidA-fsKaiB K_d, calculated as $\mathrm{kKidA_{off}}/\mathrm{kKidA_{on}}$). The resulting correlation matrix for the simulation with log likelihood L_1, which permits larger variation in the period and amplitude slopes, is shown in Figure S8A. The two parameters that were most strongly correlated with the period slope are plotted in Figures S8B and S8C.

In Figure S10, we explore the hypothesis that the effect of KidA can be approximated by shifting the equilibrium between the ground state and fold switched forms of KaiB. To do so, we performed simulations in a model without KidA, where the interconversion of the gsKaiB and fsKaiB folds was directly altered by changing the fold switching rate constants ($\mathrm{kBswitch_f}$ and $\mathrm{kBswitch_r}$), which we refer to as the effective KidA model. The simulations were run for 400 hours with a 5 μL volume reaction, 1.2 μM KaiA dimers, 1.2 μM KaiC hexamers, 4.8 μM KaiB monomers, and 0 μM KidA. The fold switching rates constants were varied uniformly on a base 10 logarithmic scale from –5 to 5 in increments of 0.5; the values of other parameters were the same as those listed in Table 4.

Supplementary figures

A

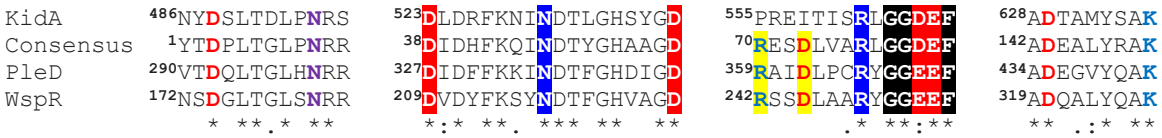

B

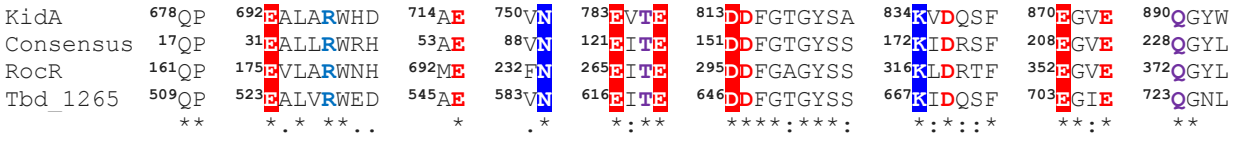

Figure S1: KidA is a putative diguanylate cyclase/phosphodiesterase

(A) Multiple sequence alignment of KidA protein sequence, the consensus sequence of the GGDEF domain, and two representative GGDEF domain-containing proteins PleD from *Caulobacter vibrioides* and WspR from *Pseudomonas aeruginosa.*

(B) Multiple sequence alignment of KidA protein sequence, the consensus sequence of the EAL domain, and two representative EAL domain-containing proteins RocR from *Pseudomonas aeruginosa* and TBD1265 from *Thiobacillus denitrificans*.

Alignments were created using Clustal Omega (10) and annotated using the same scheme in Figure 4 in Römling *et al.* (11): active site residues required for the enzymatic activity are shown in white on a colored background, and other conserved residues near the active site residues are boldened. Yellow background indicates allosteric I site residues.

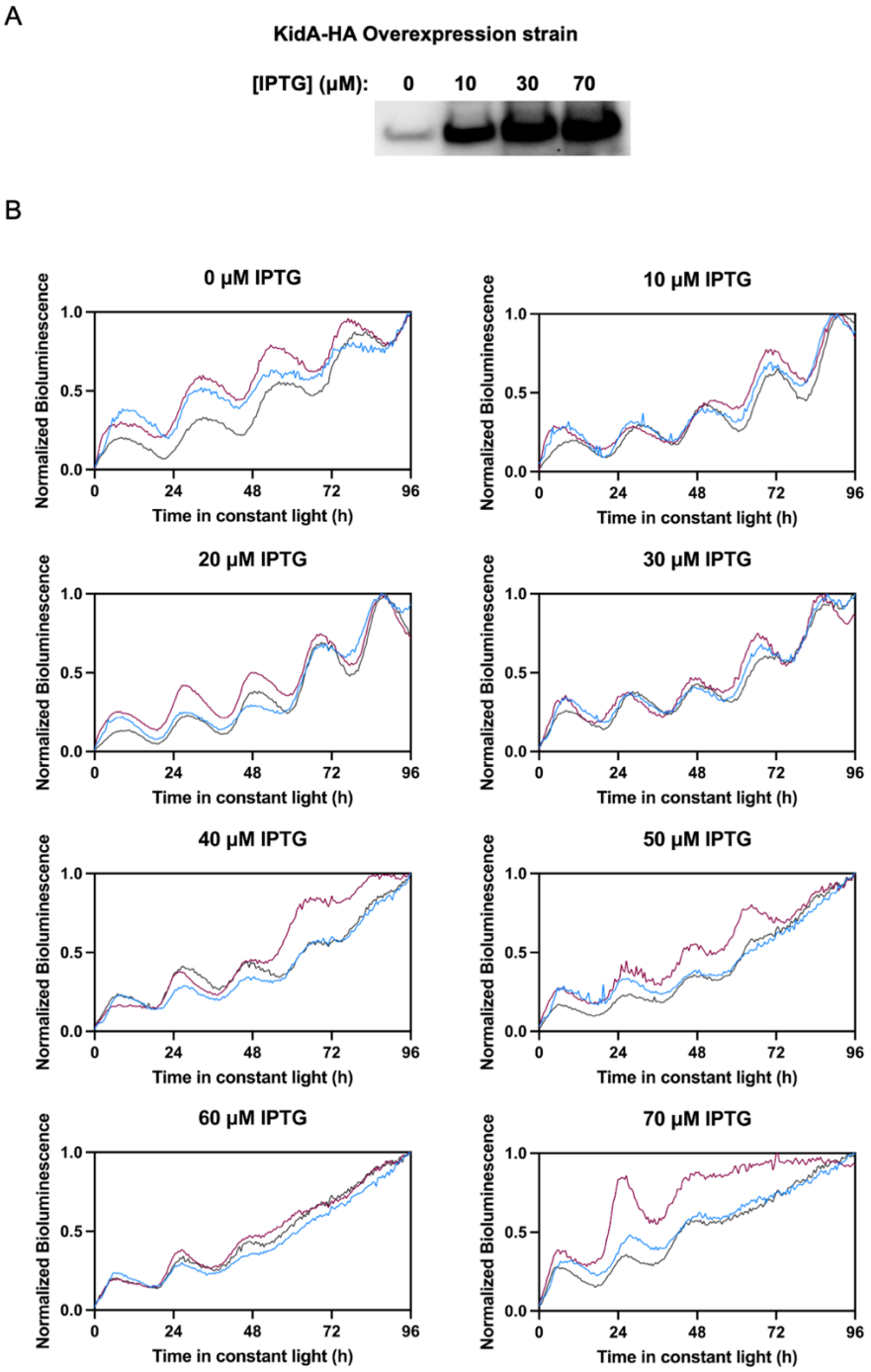

Figure S2: KidA overexpression strain has IPTG-dependent expression level of KidA protein, and high levels of IPTG induction cause arrhythmicity

(A) KidA protein expression levels of KidA overexpression strain induced without IPTG (leaky expression) or with varying concentrations of IPTG analyzed by Anti-HA Western blot.

(B) Normalized bioluminescence traces of KidA-OX reporter strain induced with 0 to 70 μM IPTG.

A

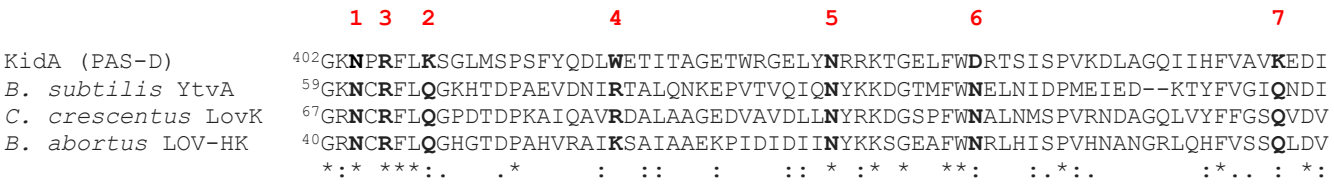

B

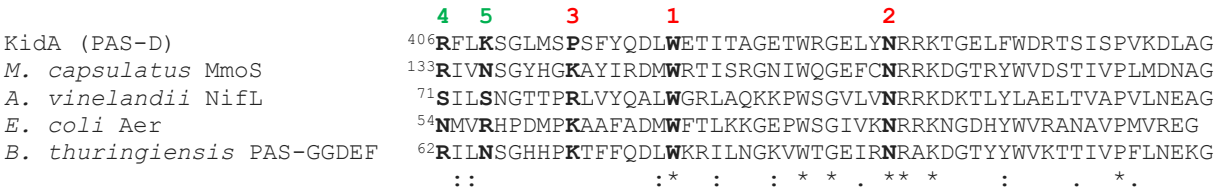

Figure S3: PAS-D alignment to LOV and MmoS/NifL domain sequences

Multiple sequence alignment of KidA protein sequence and the flavin-binding region of (A) the LOV domain sequences and (B) the MmoS and NifL domain sequences. Alignments were created using Clustal Omega (10) and annotated using the same scheme in Figure 6 and Figure 7 in a review by Henry and Crosson (12). The numbered sites are highly conserved sites that coordinate the flavin mononucleotide (FMN) and the flavin adenine dinucleotide (FAD) ligands that are noted in (12) where the structures of the active sites are described in detail.

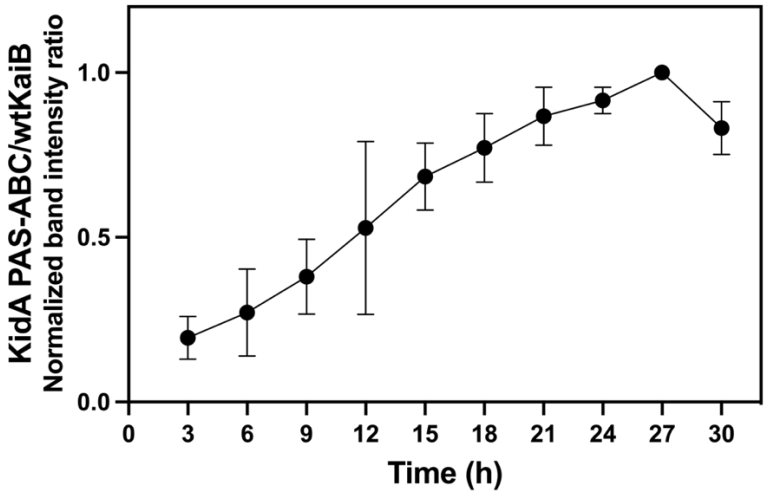

Figure S4: Kinetics of KidA PAS-ABC binding to KaiB

In vitro co-IP of KidA PAS-ABC using wtKaiB-FLAG as bait after co-incubation in 30 °C for different lengths of time. 3.5 μM KidA PAS-ABC and 3.5 μM KaiB-FLAG were used. Band intensities were determined by densitometry after background subtraction. Mean normalized band intensity ratios are plotted. Error bars show the standard deviation (N=3 for each timepoint).

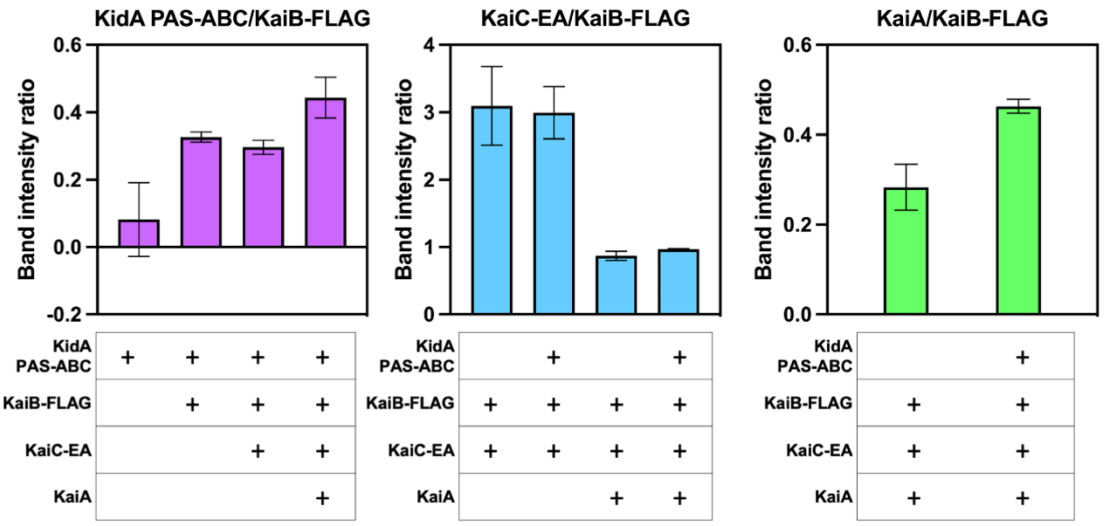

Figure S5: No obvious inhibition of Kai complex assembly caused by KidA PAS-ABC

In vitro co-IP of KaiB binding partners KidA PAS-ABC, KaiC-EA, and KaiA after 20 h co-incubation of different combinations. Band intensities were determined by densitometry after background subtraction. Mean band intensity ratios are plotted. Error bars show the standard deviation (N=3 for each condition).

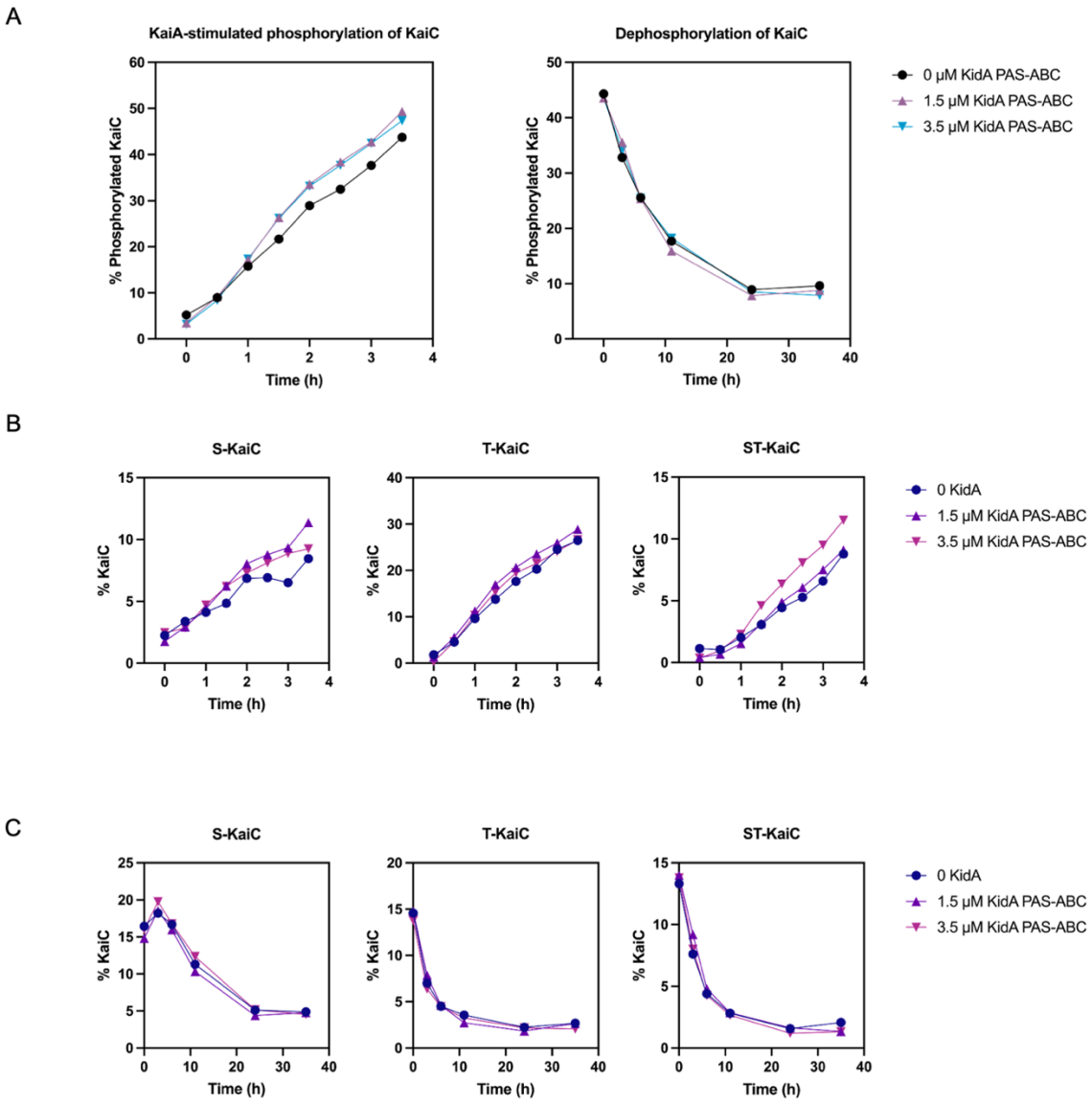

Figure S6: KidA PAS-ABC does not noticeably affect KaiA-stimulated phosphorylation and dephosphorylation of KaiC *in vitro*

(A) *Left:* The fraction of phosphorylated KaiC in KaiA-stimulated KaiC phosphorylation reactions containing 0, 1.5 μM, or 3.5 μM KidA PAS-ABC and 0.4 μM KaiA, starting from dephosphorylated KaiC at t = 0. *Right*: The fraction of phosphorylated KaiC in reactions containing 0, 1.5 μM, and 3.5 μM KidA PAS-ABC, starting from KaiC thawed from -80 °C storage at t = 0.

(B) Fraction of each phosphoform in the KaiA-stimulated KaiC phosphorylation reactions containing 0, 1.5 μM, or 3.5 μM KidA PAS-ABC, analyzed by SDS-PAGE.

(C) Fraction of each phosphoform in the KaiC dephosphorylation reactions, analyzed by SDS-PAGE.

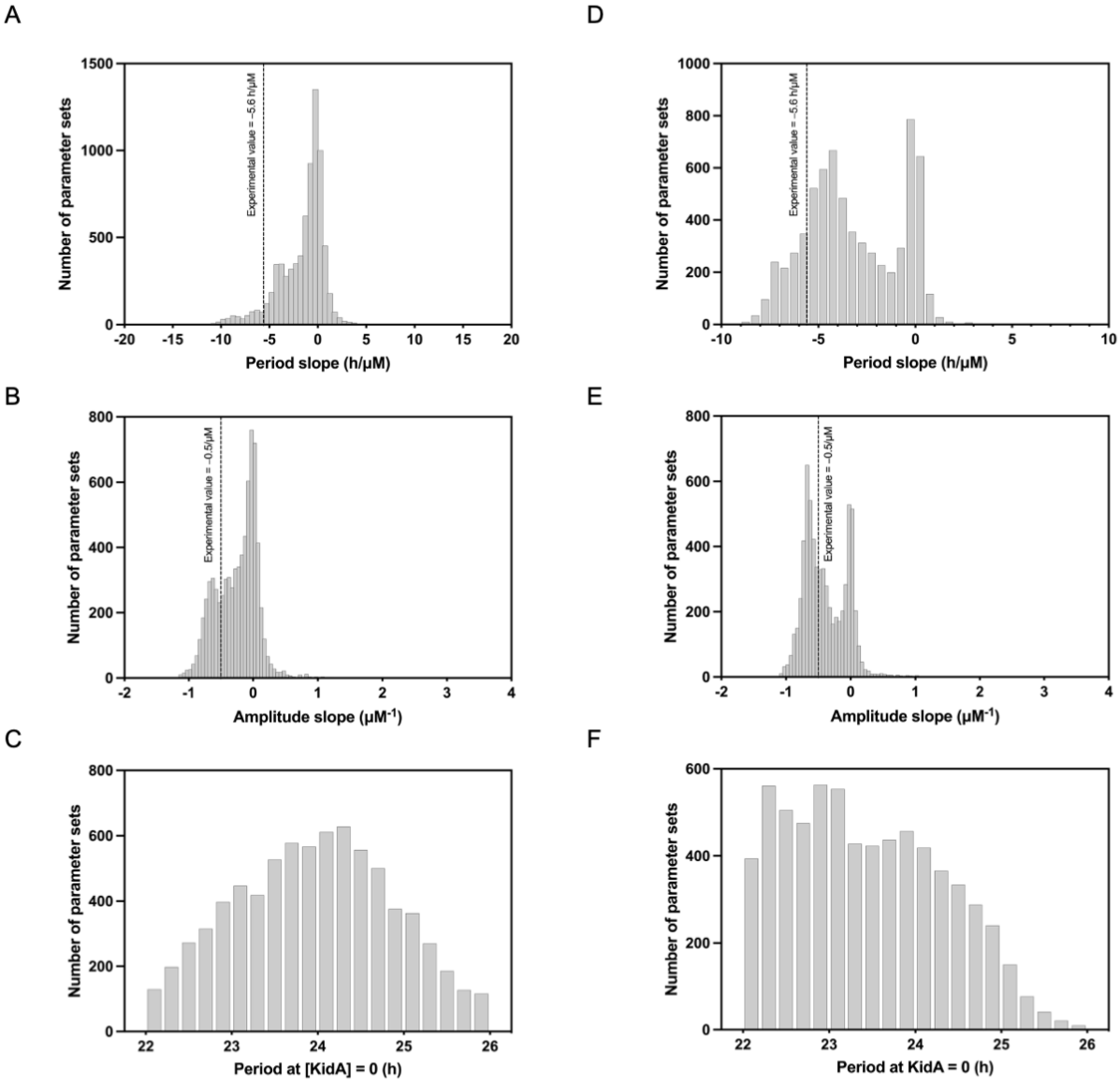

Figure S7: Dependence of the period and the amplitude on KidA concentration for sampled parameter sets

(A, D) Histogram of model slope of the period as a function of [KidA] using log likelihoods (A) L_1 and (D) L_2. The experimental slope is –5.6 h/μM.

(B, E) Histogram of model slope of the normalized amplitude as a function of [KidA] using log likelihoods (B) $L_1$and (E) L_2. The experimental slope is –0.5 /μM.

(C, F) Histogram of model period without KidA present using log likelihoods (C) L_1 and (F) L_2.

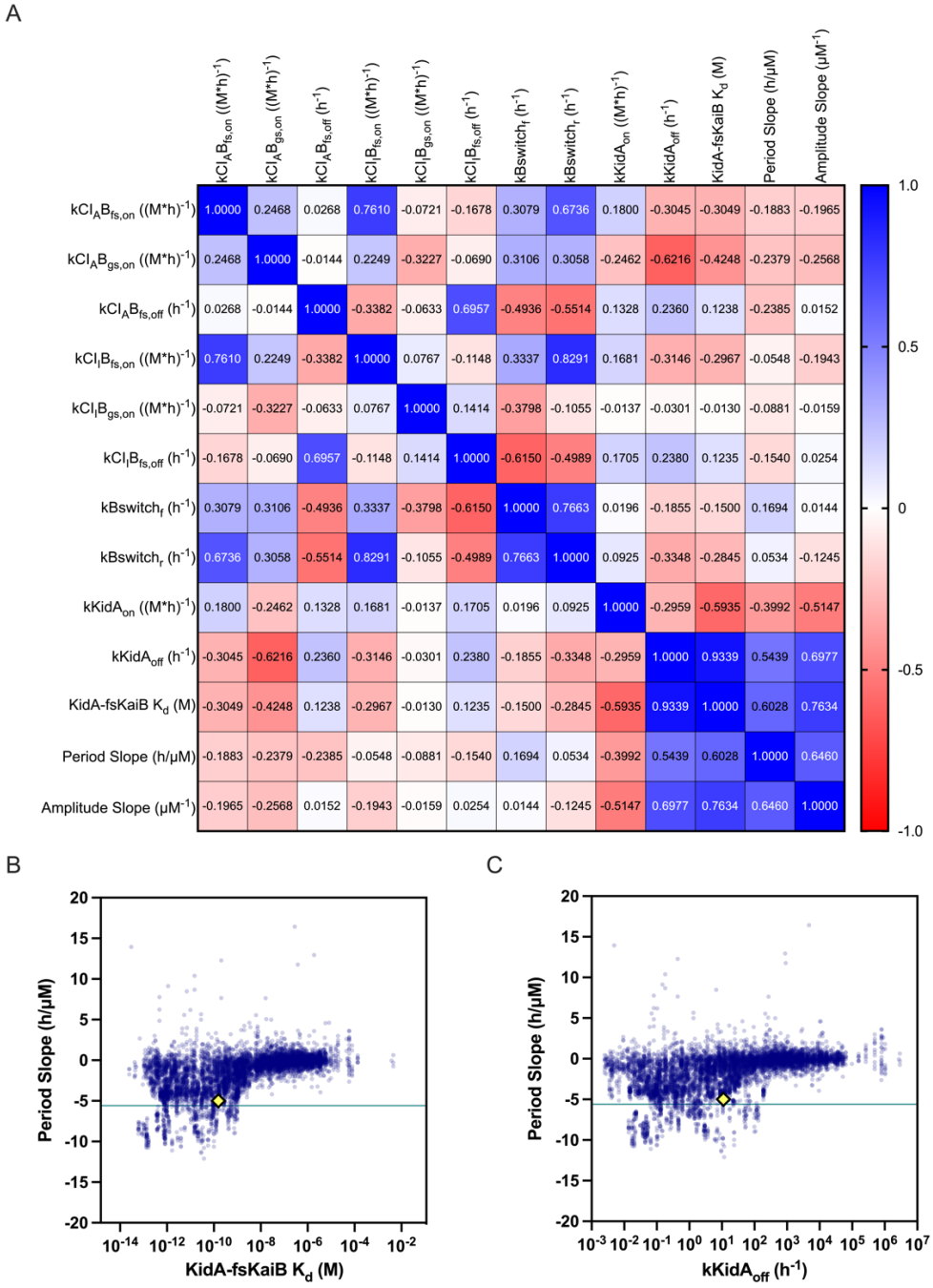

Figure S8: Correlation of model parameters with the slopes of the period and amplitude

(A) Spearman's correlation coefficient between pairs of parameters and the period and amplitude slopes.

(B) KidA-fsKaiB dissociation constant (KidA-fsKaiB Kd) and the slope of the period as a function of [KidA] for all sampled parameter sets.

(C) KidA-fsKaiB off-rate (kKidAoff) and the slope of the period as a function of [KidA] for all sampled parameter sets.

Results shown are obtained with log likelihood L_1. (B-C) The parameter set used for Figures 4C-D is marked with a yellow diamond. The horizontal line shows the experimental period slope value.

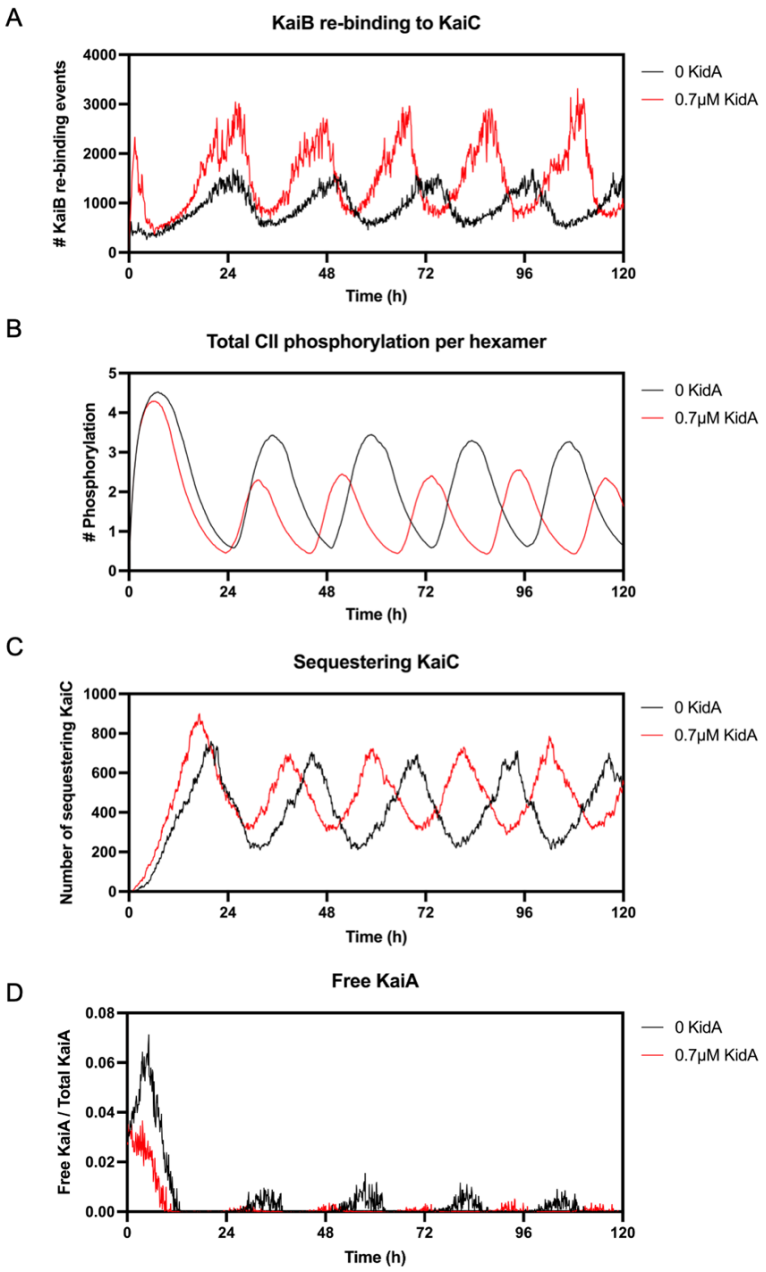

Figure S9: KidA promotes KaiB re-binding to KaiC, which alters the dynamics of phosphorylation in the model.

(A) The number of fsKaiB re-binding events for various concentrations of KidA. Binding events in which fsKaiB molecules that have previously unbound from the CI domain but have not reverted to gsKaiB bind to CI are counted every 0.1 hours.
(B) Phosphorylation per hexamer in the full oscillator reaction for indicated concentrations of KidA. Curves shown are the average numbers of subunits per KaiC hexamer that have at least one of S431 or T432 phosphorylated.
(C) The copy numbers of sequestering KaiC for various concentrations of KidA. Sequestering KaiC hexamers are KaiC hexamers with the maximal amount (6) of KaiB bound to the CI domain.
(D) The fraction of KaiA that is free in solution for various concentrations of KidA.

Simulation parameters are the same as in Figures 4C-D (SI Table 4).

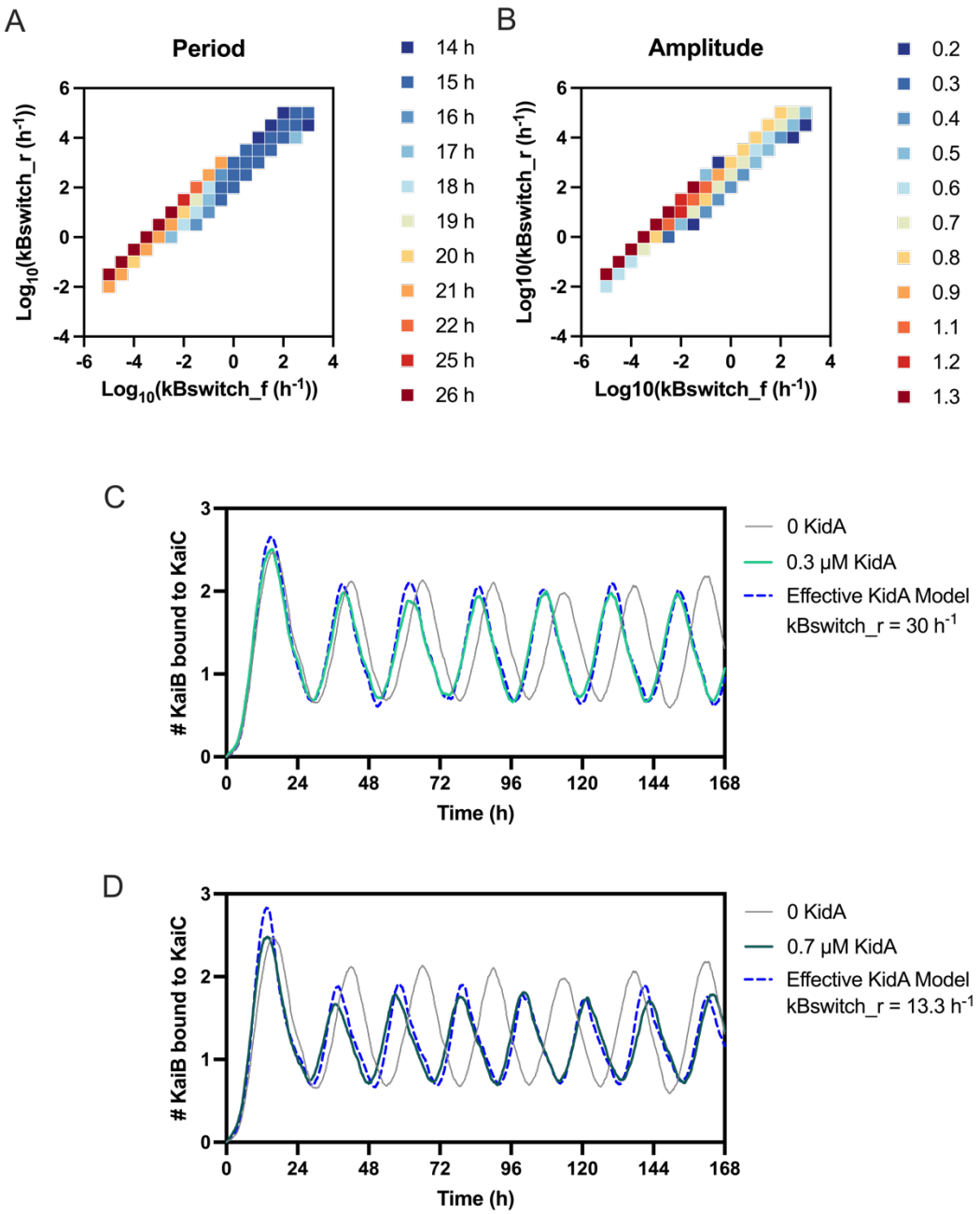

Figure S10: Shifting the equilibrium between the ground state and fold switched forms of KaiB alters the period and amplitude

(A-B) Period and amplitude of the oscillator as a function of KaiB fold switching rates in the effective KidA model (KidA is not explicitly present). Combinations of the fold switching rate that failed to produce oscillations were not plotted. That similar periods and amplitudes are obtained along the diagonal suggests that the ratio of the parameters on the axes (i.e., the equilibrium constant) is constrained but their absolute values are not.

(C-D) For comparison, two representative time courses of KaiC-bound KaiB in the effective KidA model with $\mathrm{kBswitch_r}$ decreased from 43 h^{-1} to 30 h^{-1} (C) and with $\mathrm{kBswitch_r}$ decreased from 43 h^{-1} to 13.3 h^{-1} (D) are shown together with time courses of KaiC-bound KaiB from the full model with 0.3 μM KidA and 0.7 μM KidA, respectively.

Supplementary Information Tables

Supplementary Information Table 1: Strains information

Strain name	Plasmid used	Background strain	Antibiotic resistance	First residue	Last residue
fsKaiB-HA (MRC1109)	MR0114	WT Syn7942	Spec	N/A	N/A
Δ*kidA* (MRC1180)	MR0213	WT/pAM2195	Cm, Gent	N/A	N/A
KidA FL (MRC1185)	MR0214	WT/pAM2195	Cm, Spec	1M	917S
KidA PAS-ABCD (MRC1204)	MR0222	WT/pAM2195	Cm, Spec	1M	485A
KidA PAS-ABC (MRC1205)	MR0223	WT/pAM2195	Cm, Spec	1M	359L
KidA PAS-BCD (MRC1200)	MR0220	WT/pAM2195	Cm, Spec	131L	485A
KidA PAS-AB (MRC 1227)	MR0226	WT/pAM2195	Cm, Spec	1M	254Q
KidA PAS-A (MRC1207)	MR0224	WT/pAM2195	Cm, Spec	1M	130Q

Supplementary Information Table 2

List of proteins detected in co-IP/MS experiment performed using fsKaiB as bait in light (L) condition

Rank	Accession	Description	Area
1	Q79PF4	Circadian clock protein kinase KaiC OS=Synechococcus elongatus (strain PCC 7942) GN=kaiC PE=1 SV=1	6.78E+09
2	Q79PF5	Circadian clock protein KaiB OS=Synechococcus elongatus (strain PCC 7942) GN=kaiB PE=1 SV=1	1.96E+09
3	Q31M30	Diguanylate cyclase/phosphodiesterase with PAS/PAC sensor(S) OS=Synechococcus elongatus (strain PCC 7942) GN=Synpcc7942_1859 PE=4 SV=1	1.78E+08
4	Q79PF6	Circadian clock protein KaiA OS=Synechococcus elongatus (strain PCC 7942) GN=kaiA PE=1 SV=1	8.52E+07
5	Q31NT0	Arsenite-activated ATPase (ArsA) OS=Synechococcus elongatus (strain PCC 7942) GN=Synpcc7942_1259 PE=4 SV=1	6.68E+07
6	Q31Q47	RNA-binding region RNP-1 OS=Synechococcus elongatus (strain PCC 7942) GN=Synpcc7942_0790 PE=4 SV=1	5.55E+07
7	Q31KS4	ATP synthase subunit beta OS=Synechococcus elongatus (strain PCC 7942) GN=atpD PE=3 SV=1	3.39E+07
8	Q31LF9	Probable phosphoketolase OS=Synechococcus elongatus (strain PCC 7942) GN=Synpcc7942_2080 PE=3 SV=1	2.44E+07
9	Q31PZ1	Twitching motility protein OS=Synechococcus elongatus (strain PCC 7942) GN=Synpcc7942_0847 PE=4 SV=1	2.41E+07
10	Q31KP0	Twitching motility protein OS=Synechococcus elongatus (strain PCC 7942) GN=Synpcc7942_2349 PE=4 SV=1	2.29E+07
11	Q31KE3	Methionine aminopeptidase OS=Synechococcus elongatus (strain PCC 7942) GN=map PE=3 SV=1	2.26E+07
12	Q31K60	Uncharacterized protein OS=Synechococcus elongatus (strain PCC 7942) GN=Synpcc7942_2529 PE=4 SV=1	1.97E+07
13	Q31PH5	CheA signal transduction histidine kinase OS=Synechococcus elongatus (strain PCC 7942) GN=Synpcc7942_1014 PE=4 SV=1	1.95E+07
14	Q31MB3	Uncharacterized protein OS=Synechococcus elongatus (strain PCC 7942) GN=Synpcc7942_1776 PE=4 SV=1	1.93E+07
15	Q93AK0	Cell division protein Ftn2 OS=Synechococcus elongatus (strain PCC 7942) GN=Synpcc7942_1943 PE=4 SV=1	1.92E+07
16	Q54775	CTP synthase OS=Synechococcus elongatus (strain PCC 7942) GN=pyrG PE=3 SV=1	1.70E+07
17	Q31QF2	60 kDa chaperonin OS=Synechococcus elongatus (strain PCC 7942) GN=groL PE=3 SV=1	1.69E+07
18	Q31N20	Histidinol dehydrogenase OS=Synechococcus elongatus (strain PCC 7942) GN=hisD PE=3 SV=1	1.67E+07
19	Q9Z3G5	PBS lyase HEAT-like repeat OS=Synechococcus elongatus (strain PCC 7942) GN=nblB PE=4 SV=1	1.46E+07
20	Q8GAA4	Uncharacterized protein OS=Synechococcus elongatus (strain PCC 7942) GN=sek0026 PE=4 SV=1	1.39E+07
21	Q31PX1	Uncharacterized protein OS=Synechococcus elongatus (strain PCC 7942) GN=Synpcc7942_0868 PE=4 SV=1	1.27E+07
22	P11004	Photosystem II CP43 reaction center protein OS=Synechococcus elongatus (strain PCC 7942) GN=psbC PE=3 SV=3	1.25E+07

23	Q31K58	Elongation factor Ts OS=Synechococcus elongatus (strain PCC 7942) GN=tsf PE=3 SV=1	1.25E+07
24	Q31KE8	Phosphate import ATP-binding protein PstB OS=Synechococcus elongatus (strain PCC 7942) GN=pstB PE=3 SV=1	1.18E+07
25	P22880	10 kDa chaperonin OS=Synechococcus elongatus (strain PCC 7942) GN=groS PE=3 SV=2	1.13E+07
26	Q31RF6	ATP synthase subunit a OS=Synechococcus elongatus (strain PCC 7942) GN=atpB PE=3 SV=2	1.12E+07
27	Q31LR4	Uncharacterized protein OS=Synechococcus elongatus (strain PCC 7942) GN=Synpcc7942_1975 PE=4 SV=1	1.11E+07
28	Q8GJN0	Light-independent protochlorophyllide reductase subunit B OS=Synechococcus elongatus (strain PCC 7942) GN=chlB PE=3 SV=2	1.05E+07
29	Q31NI8	HAD-superfamily hydrolase subfamily IA, variant 3 OS=Synechococcus elongatus (strain PCC 7942) GN=Synpcc7942_1351 PE=4 SV=1	1.01E+07
30	Q31RH4	Uncharacterized protein OS=Synechococcus elongatus (strain PCC 7942) GN=Synpcc7942_0313 PE=4 SV=1	1.00E+07
31	Q31RX9	Rhodanese-like OS=Synechococcus elongatus (strain PCC 7942) GN=Synpcc7942_0158 PE=4 SV=1	8.99E+06
32	Q31PA8	Uncharacterized protein OS=Synechococcus elongatus (strain PCC 7942) GN=Synpcc7942_1081 PE=4 SV=1	8.77E+06
33	Q31P08	NAD(P)H-quinone oxidoreductase subunit K OS=Synechococcus elongatus (strain PCC 7942) GN=ndhK PE=3 SV=1	8.62E+06
34	Q8KPQ7	Guanylate kinase OS=Synechococcus elongatus (strain PCC 7942) GN=gmk PE=3 SV=2	8.43E+06
35	Q31MD1	Probable dual-specificity RNA methyltransferase RlmN OS=Synechococcus elongatus (strain PCC 7942) GN=rlmN PE=3 SV=1	8.39E+06
36	Q54766	Acetyl-coenzyme A carboxylase carboxyl transferase subunit alpha OS=Synechococcus elongatus (strain PCC 7942) GN=accA PE=3 SV=1	8.24E+06
37	Q31NA4	2-succinyl-5-enolpyruvyl-6-hydroxy-3-cyclohexene-1-carboxylate synthase OS=Synechococcus elongatus (strain PCC 7942) GN=menD PE=3 SV=1	8.24E+06
38	Q31PX7	Uncharacterized protein OS=Synechococcus elongatus (strain PCC 7942) GN=Synpcc7942_0862 PE=4 SV=1	7.27E+06
39	Q31MP2	Uncharacterized protein OS=Synechococcus elongatus (strain PCC 7942) GN=Synpcc7942_1647 PE=4 SV=1	7.25E+06
40	Q31LF8	Probable glycosyl transferase OS=Synechococcus elongatus (strain PCC 7942) GN=Synpcc7942_2081 PE=4 SV=1	7.24E+06
41	Q31N30	tRNA-specific 2-thiouridylase MnmA OS=Synechococcus elongatus (strain PCC 7942) GN=mnmA PE=3 SV=1	7.23E+06
42	P21577	6-phosphogluconate dehydrogenase, decarboxylating OS=Synechococcus elongatus (strain PCC 7942) GN=gnd PE=1 SV=4	7.18E+06
43	Q31KH4	Lysine--tRNA ligase OS=Synechococcus elongatus (strain PCC 7942) GN=lysS PE=3 SV=1	7.08E+06
44	Q54734	SqdB OS=Synechococcus elongatus (strain PCC 7942) GN=sqdB PE=4 SV=1	6.91E+06
45	Q31KY2	Uncharacterized protein OS=Synechococcus elongatus (strain PCC 7942) GN=Synpcc7942_2257 PE=4 SV=1	6.85E+06
46	Q31Q29	HAD-superfamily hydrolase subfamily IIB OS=Synechococcus elongatus (strain PCC 7942) GN=Synpcc7942_0808 PE=4 SV=1	6.76E+06
47	Q31M14	Uncharacterized protein OS=Synechococcus elongatus (strain PCC 7942) GN=Synpcc7942_1875 PE=4 SV=1	6.70E+06
48	Q8VPV7	CO2 hydration protein OS=Synechococcus elongatus (strain PCC 7942) GN=chpY PE=4 SV=1	6.61E+06
49	Q31KY3	Uncharacterized protein OS=Synechococcus elongatus (strain PCC 7942) GN=Synpcc7942_2256 PE=4 SV=1	6.48E+06
50	Q31QQ2	PDZ/DHR/GLGF OS=Synechococcus elongatus (strain PCC 7942) GN=Synpcc7942_0585 PE=4 SV=1	6.21E+06
51	Q31RD2	Ribosome-binding factor A OS=Synechococcus elongatus (strain PCC 7942) GN=rbfA PE=3 SV=1	6.12E+06
52	Q935Z3	Trigger factor OS=Synechococcus elongatus (strain PCC 7942) GN=tig PE=3 SV=1	6.10E+06
53	Q31NJ4	NADH dehydrogenase subunit 6 OS=Synechococcus elongatus (strain PCC 7942) GN=Synpcc7942_1345 PE=3 SV=1	6.09E+06
54	P52023	DNA polymerase III subunit beta OS=Synechococcus elongatus (strain PCC 7942) GN=dnaN PE=3 SV=1	6.08E+06
55	Q31NF8	ATPase OS=Synechococcus elongatus (strain PCC 7942) GN=Synpcc7942_1381 PE=4 SV=1	5.94E+06
56	Q31LE9	Homoserine dehydrogenase OS=Synechococcus elongatus (strain PCC 7942) GN=Synpcc7942_2090 PE=3 SV=1	5.91E+06
57	Q31RI3	Uncharacterized protein OS=Synechococcus elongatus (strain PCC 7942) GN=Synpcc7942_0304 PE=4 SV=1	5.87E+06
58	Q31MS2	Inner membrane protein-like OS=Synechococcus elongatus (strain PCC 7942) GN=Synpcc7942_1617 PE=3 SV=1	5.84E+06
59	Q31N89	ATPase OS=Synechococcus elongatus (strain PCC 7942) GN=Synpcc7942_1450 PE=4 SV=1	5.76E+06
60	O05347	MalK-like protein OS=Synechococcus elongatus (strain PCC 7942) GN=cynD PE=4 SV=2	5.74E+06
61	Q935Y2	Ribosomal protein S12 methylthiotransferase RimO OS=Synechococcus elongatus (strain PCC 7942) GN=rimO PE=3 SV=1	5.70E+06

62	Q31M19	Secretion protein HlyD OS=Synechococcus elongatus (strain PCC 7942) GN=Synpcc7942_1870 PE=3 SV=1	5.58E+06
63	Q31S00	Ferrochelatase OS=Synechococcus elongatus (strain PCC 7942) GN=hemH PE=3 SV=1	5.45E+06
64	Q31QN3	Ribulose-phosphate 3-epimerase OS=Synechococcus elongatus (strain PCC 7942) GN=Synpcc7942_0604 PE=3 SV=1	5.27E+06
65	P50020	Chaperone protein dnaK1 OS=Synechococcus elongatus (strain PCC 7942) GN=dnaK1 PE=3 SV=2	5.26E+06
66	Q31PP8	ATPase OS=Synechococcus elongatus (strain PCC 7942) GN=Synpcc7942_0941 PE=4 SV=1	5.23E+06
67	Q31LG9	Twitching motility protein OS=Synechococcus elongatus (strain PCC 7942) GN=Synpcc7942_2070 PE=4 SV=1	5.22E+06
68	Q31S36	Type 2 NADH dehydrogenase OS=Synechococcus elongatus (strain PCC 7942) GN=Synpcc7942_0101 PE=4 SV=1	5.18E+06
69	Q31NL4	Replicative DNA helicase OS=Synechococcus elongatus (strain PCC 7942) GN=Synpcc7942_1325 PE=3 SV=1	5.17E+06
70	Q31L91	ATPase OS=Synechococcus elongatus (strain PCC 7942) GN=Synpcc7942_2148 PE=4 SV=1	5.16E+06
71	Q31PV4	Elongation factor G OS=Synechococcus elongatus (strain PCC 7942) GN=fusA PE=3 SV=1	5.04E+06
72	Q31QI3	Photosystem I assembly protein Ycf4 OS=Synechococcus elongatus (strain PCC 7942) GN=ycf4 PE=3 SV=1	4.96E+06
73	Q31QL1	Dihydroxy-acid dehydratase OS=Synechococcus elongatus (strain PCC 7942) GN=ilvD PE=3 SV=1	4.92E+06
74	Q31P87	Uncharacterized protein OS=Synechococcus elongatus (strain PCC 7942) GN=Synpcc7942_1102 PE=4 SV=1	4.87E+06
75	Q31SB1	Uncharacterized protein OS=Synechococcus elongatus (strain PCC 7942) GN=Synpcc7942_0026 PE=4 SV=1	4.63E+06
76	Q31KR9	Uncharacterized protein OS=Synechococcus elongatus (strain PCC 7942) GN=Synpcc7942_2320 PE=4 SV=1	4.59E+06
77	Q31K23	Peptidyl-prolyl cis-trans isomerase OS=Synechococcus elongatus (strain PCC 7942) GN=Synpcc7942_2566 PE=4 SV=1	4.44E+06
78	Q31PV7	Peptidase S16, lon-like OS=Synechococcus elongatus (strain PCC 7942) GN=Synpcc7942_0882 PE=4 SV=1	4.43E+06
79	Q31LY0	Uncharacterized protein OS=Synechococcus elongatus (strain PCC 7942) GN=Synpcc7942_1909 PE=4 SV=1	4.41E+06
80	Q31RE1	Laccase domain protein OS=Synechococcus elongatus (strain PCC 7942) GN=Synpcc7942_0346 PE=3 SV=1	4.37E+06
81	Q8KUT3	ANL58 OS=Synechococcus elongatus (strain PCC 7942) GN=Synpcc7942_B2655 PE=4 SV=2	4.33E+06
82	Q31NN4	ATPase OS=Synechococcus elongatus (strain PCC 7942) GN=Synpcc7942_1305 PE=3 SV=1	4.21E+06
83	Q31RS6	Cobyric acid synthase OS=Synechococcus elongatus (strain PCC 7942) GN=cobQ PE=3 SV=1	4.20E+06
84	Q9KHI5	Circadian input kinase OS=Synechococcus elongatus (strain PCC 7942) GN=cikA PE=1 SV=1	4.19E+06
85	Q31NI3	Response regulator receiver domain protein (CheY-like) OS=Synechococcus elongatus (strain PCC 7942) GN=Synpcc7942_1356 PE=4 SV=1	4.06E+06
86	Q31QA3	Uncharacterized protein OS=Synechococcus elongatus (strain PCC 7942) GN=Synpcc7942_0734 PE=4 SV=1	3.99E+06
87	P14788	Sulfate/thiosulfate import ATP-binding protein CysA OS=Synechococcus elongatus (strain PCC 7942) GN=cysA PE=2 SV=1	3.94E+06
88	Q31NF3	Cob(I)yrinic acid a,c-diamide adenosyltransferase OS=Synechococcus elongatus (strain PCC 7942) GN=Synpcc7942_1386 PE=4 SV=1	3.93E+06
89	Q31Q03	Holliday junction ATP-dependent DNA helicase RuvB OS=Synechococcus elongatus (strain PCC 7942) GN=ruvB PE=3 SV=1	3.88E+06
90	Q31LC0	RNA methyltransferase TrmH, group 3 OS=Synechococcus elongatus (strain PCC 7942) GN=Synpcc7942_2119 PE=3 SV=1	3.82E+06
91	Q8GMQ9	Putative glutathione peroxidase OS=Synechococcus elongatus (strain PCC 7942) GN=sel0033 PE=4 SV=1	3.67E+06
92	Q31QZ9	Dihydroorotase OS=Synechococcus elongatus (strain PCC 7942) GN=Synpcc7942_0488 PE=3 SV=1	3.55E+06
93	Q31LU5	Pyruvate dehydrogenase E1 component subunit alpha OS=Synechococcus elongatus (strain PCC 7942) GN=pdhA PE=4 SV=1	3.54E+06
94	Q31LY5	Hemolysin secretion protein-like OS=Synechococcus elongatus (strain PCC 7942) GN=Synpcc7942_1904 PE=4 SV=1	3.50E+06
95	O07345	Magnesium-chelatase subunit ChlD OS=Synechococcus elongatus (strain PCC 7942) GN=chlD PE=3 SV=2	3.46E+06
96	Q31NH7	Uncharacterized protein OS=Synechococcus elongatus (strain PCC 7942) GN=Synpcc7942_1362 PE=4 SV=1	3.43E+06
97	Q31RH2	Adenylosuccinate lyase OS=Synechococcus elongatus (strain PCC 7942) GN=Synpcc7942_0315 PE=3 SV=1	3.35E+06
98	Q31QS3	ATPase OS=Synechococcus elongatus (strain PCC 7942) GN=Synpcc7942_0564 PE=4 SV=1	3.33E+06
99	Q31KG6	tRNA uridine 5-carboxymethylaminomethyl modification enzyme MnmG OS=Synechococcus elongatus (strain PCC 7942) GN=mnmG PE=3 SV=1	3.29E+06
100	Q31LN3	Uncharacterized protein OS=Synechococcus elongatus (strain PCC 7942) GN=Synpcc7942_2006 PE=4 SV=1	3.23E+06

101	Q8GJM5	Putative uncharacterized protein SEN0014 OS=Synechococcus elongatus (strain PCC 7942) GN=SEN0014 PE=4 SV=1	3.17E+06
102	Q31K73	Uncharacterized protein OS=Synechococcus elongatus (strain PCC 7942) GN=Synpcc7942_2516 PE=4 SV=1	3.04E+06
103	Q31NE8	Mg chelatase-related protein OS=Synechococcus elongatus (strain PCC 7942) GN=Synpcc7942_1391 PE=4 SV=1	2.98E+06
104	Q31Q32	Uncharacterized protein OS=Synechococcus elongatus (strain PCC 7942) GN=Synpcc7942_0805 PE=4 SV=1	2.92E+06
105	Q8GMT4	Preprotein translocase, SecG subunit OS=Synechococcus elongatus (strain PCC 7942) GN=secG PE=4 SV=1	2.89E+06
106	Q31R08	Elongation factor 4 OS=Synechococcus elongatus (strain PCC 7942) GN=lepA PE=3 SV=1	2.82E+06
107	Q31LN9	Penicillin-binding protein 1A OS=Synechococcus elongatus (strain PCC 7942) GN=Synpcc7942_2000 PE=4 SV=1	2.67E+06
108	Q935X4	ChlA OS=Synechococcus elongatus (strain PCC 7942) GN=SEA0022 PE=4 SV=1	2.60E+06
109	Q31PZ6	NADPH-glutathione reductase OS=Synechococcus elongatus (strain PCC 7942) GN=Synpcc7942_0842 PE=3 SV=1	2.58E+06
110	Q31L26	Adenylate kinase OS=Synechococcus elongatus (strain PCC 7942) GN=adk PE=3 SV=1	2.47E+06
111	Q56002	Serine acetyltransferase OS=Synechococcus elongatus (strain PCC 7942) GN=cysE PE=3 SV=1	2.47E+06
112	Q31NI0	Coenzyme F420 hydrogenase OS=Synechococcus elongatus (strain PCC 7942) GN=Synpcc7942_1359 PE=4 SV=1	2.38E+06
113	Q8RQ68	Multi-sensor signal transduction histidine kinase OS=Synechococcus elongatus (strain PCC 7942) GN=nblS PE=4 SV=1	2.30E+06
114	Q31PS7	DNA polymerase III, tau subunit OS=Synechococcus elongatus (strain PCC 7942) GN=Synpcc7942_0912 PE=4 SV=1	2.27E+06
115	P37279	Probable copper-transporting ATPase PacS OS=Synechococcus elongatus (strain PCC 7942) GN=pacS PE=3 SV=2	2.17E+06
116	P50590	Nucleoside diphosphate kinase OS=Synechococcus elongatus (strain PCC 7942) GN=ndk PE=3 SV=2	2.04E+06
117	P11005	Photosystem II D2 protein OS=Synechococcus elongatus (strain PCC 7942) GN=psbD1 PE=3 SV=2	2.03E+06
118	Q31KU4	Uncharacterized protein OS=Synechococcus elongatus (strain PCC 7942) GN=Synpcc7942_2295 PE=4 SV=1	2.02E+06
119	Q31M79	Flavoprotein OS=Synechococcus elongatus (strain PCC 7942) GN=Synpcc7942_1810 PE=4 SV=1	1.98E+06
120	Q31KI0	Adenylosuccinate synthetase OS=Synechococcus elongatus (strain PCC 7942) GN=purA PE=3 SV=1	1.97E+06
121	Q31RV9	ATPase OS=Synechococcus elongatus (strain PCC 7942) GN=Synpcc7942_0178 PE=4 SV=1	1.95E+06
122	Q31KN9	Translation factor SUA5 OS=Synechococcus elongatus (strain PCC 7942) GN=Synpcc7942_2350 PE=4 SV=1	1.92E+06
123	Q31M41	Aspartate-semialdehyde dehydrogenase OS=Synechococcus elongatus (strain PCC 7942) GN=asd PE=3 SV=1	1.92E+06
124	Q31S19	Aspartyl/glutamyl-tRNA(Asn/Gln) amidotransferase subunit B OS=Synechococcus elongatus (strain PCC 7942) GN=gatB PE=3 SV=1	1.89E+06
125	Q31KE1	GTPase HflX OS=Synechococcus elongatus (strain PCC 7942) GN=hflX PE=3 SV=1	1.76E+06
126	Q31QJ5	Bacterioferritin comigratory protein OS=Synechococcus elongatus (strain PCC 7942) GN=Synpcc7942_0642 PE=4 SV=1	1.73E+06
127	Q31MA7	L-threonine synthase OS=Synechococcus elongatus (strain PCC 7942) GN=Synpcc7942_1782 PE=4 SV=1	1.53E+06
128	Q31RX7	GTPase Era OS=Synechococcus elongatus (strain PCC 7942) GN=era PE=3 SV=1	1.52E+06
129	Q31LE3	Diguanylate cyclase with GAF sensor OS=Synechococcus elongatus (strain PCC 7942) GN=Synpcc7942_2096 PE=4 SV=1	1.50E+06
130	Q55041	Phosphoribosylformylglycinamidine synthase subunit PurL OS=Synechococcus elongatus (strain PCC 7942) GN=purL PE=3 SV=3	1.49E+06
131	Q31MB0	DNA repair protein RecN OS=Synechococcus elongatus (strain PCC 7942) GN=Synpcc7942_1779 PE=3 SV=1	1.47E+06
132	Q31Q56	Phosphoenolpyruvate synthase OS=Synechococcus elongatus (strain PCC 7942) GN=Synpcc7942_0781 PE=3 SV=1	1.43E+06
133	Q31RJ4	Uncharacterized protein OS=Synechococcus elongatus (strain PCC 7942) GN=Synpcc7942_0293 PE=4 SV=1	1.40E+06
134	Q31P89	Chromosomal replication initiator protein DnaA OS=Synechococcus elongatus (strain PCC 7942) GN=dnaA PE=3 SV=1	1.38E+06
135	Q31LJ1	Photosystem I P700 chlorophyll a apoprotein A2 OS=Synechococcus elongatus (strain PCC 7942) GN=psaB PE=3 SV=1	1.37E+06
136	Q54769	GTP cyclohydrolase 1 OS=Synechococcus elongatus (strain PCC 7942) GN=folE PE=3 SV=2	1.33E+06
137	Q31QF4	Potassium channel protein OS=Synechococcus elongatus (strain PCC 7942) GN=Synpcc7942_0683 PE=4 SV=1	1.27E+06
138	Q31JZ3	Probable oxidoreductase OS=Synechococcus elongatus (strain PCC 7942) GN=Synpcc7942_2596 PE=4 SV=1	1.24E+06
139	Q8GLI4	Light dependent period OS=Synechococcus elongatus (strain PCC 7942) GN=ldpA PE=1 SV=1	1.22E+06

140	Q31RE4	Photosystem II lipoprotein Psb27 OS=Synechococcus elongatus (strain PCC 7942) GN=psb27 PE=3 SV=1	1.20E+06
141	Q06904	Adaptive-response sensory-kinase SasA OS=Synechococcus elongatus (strain PCC 7942) GN=sasA PE=1 SV=2	1.18E+06
142	Q31R39	Zinc metalloprotease OS=Synechococcus elongatus (strain PCC 7942) GN=Synpcc7942_0448 PE=3 SV=1	1.13E+06
143	Q31PN2	Cob(I)yrinic acid a,c-diamide adenosyltransferase OS=Synechococcus elongatus (strain PCC 7942) GN=Synpcc7942_0957 PE=4 SV=1	1.06E+06
144	Q31RJ9	Bifunctional protein GlmU OS=Synechococcus elongatus (strain PCC 7942) GN=glmU PE=3 SV=1	1.05E+06
145	Q31Q25	Heat shock protein DnaJ-like OS=Synechococcus elongatus (strain PCC 7942) GN=Synpcc7942_0812 PE=4 SV=1	1.05E+06
146	Q31PY0	CheA signal transduction histidine kinase OS=Synechococcus elongatus (strain PCC 7942) GN=Synpcc7942_0859 PE=4 SV=1	1.02E+06
147	Q31LJ0	Photosystem I P700 chlorophyll a apoprotein A1 OS=Synechococcus elongatus (strain PCC 7942) GN=psaA PE=3 SV=1	1.01E+06
148	Q31MX7	ADP-ribosylglycohydrolase-like OS=Synechococcus elongatus (strain PCC 7942) GN=Synpcc7942_1562 PE=4 SV=1	9.99E+05
149	Q31RX1	Uncharacterized protein OS=Synechococcus elongatus (strain PCC 7942) GN=Synpcc7942_0166 PE=4 SV=1	9.72E+05
150	Q31KD8	Putative type IV pilus assembly protein PilO OS=Synechococcus elongatus (strain PCC 7942) GN=Synpcc7942_2451 PE=4 SV=1	9.21E+05
151	Q31MT1	Mannose-1-phosphate guanylyltransferase (GDP) OS=Synechococcus elongatus (strain PCC 7942) GN=Synpcc7942_1608 PE=3 SV=1	8.90E+05
152	P38045	Nitrate transport ATP-binding protein NrtC OS=Synechococcus elongatus (strain PCC 7942) GN=nrtC PE=3 SV=1	8.77E+05
153	Q31LA7	Phosphoglucosamine mutase OS=Synechococcus elongatus (strain PCC 7942) GN=glmM PE=3 SV=1	7.93E+05
154	Q31NE2	Uncharacterized protein OS=Synechococcus elongatus (strain PCC 7942) GN=Synpcc7942_1397 PE=4 SV=1	6.74E+05
155	Q31KC6	S-adenosylmethionine synthase OS=Synechococcus elongatus (strain PCC 7942) GN=metK PE=3 SV=1	6.51E+05
156	Q31RW6	Cysteine synthase OS=Synechococcus elongatus (strain PCC 7942) GN=Synpcc7942_0171 PE=4 SV=1	6.30E+05
157	Q31LG1	Phosphoglycerate mutase OS=Synechococcus elongatus (strain PCC 7942) GN=Synpcc7942_2078 PE=4 SV=1	5.60E+05
158	Q31QC5	C-terminal processing peptidase-2. Serine peptidase. MEROPS family S41A OS=Synechococcus elongatus (strain PCC 7942) GN=Synpcc7942_0712 PE=3 SV=1	5.42E+05

Supplementary Information Table 3

List of proteins detected in co-IP/MS experiment performed using fsKaiB as bait in dark (D) condition

Rank	Accession	Description	Area
1	Q79PF4	Circadian clock protein kinase KaiC OS=Synechococcus elongatus (strain PCC 7942) GN=kaiC PE=1 SV=1	4.13E+09
2	Q79PF5	Circadian clock protein KaiB OS=Synechococcus elongatus (strain PCC 7942) GN=kaiB PE=1 SV=1	2.83E+08
3	Q31Q47	RNA-binding region RNP-1 OS=Synechococcus elongatus (strain PCC 7942) GN=Synpcc7942_0790 PE=4 SV=1	7.74E+07
4	Q31MB3	Uncharacterized protein OS=Synechococcus elongatus (strain PCC 7942) GN=Synpcc7942_1776 PE=4 SV=1	5.93E+07
5	Q31K58	Elongation factor Ts OS=Synechococcus elongatus (strain PCC 7942) GN=tsf PE=3 SV=1	5.43E+07
6	Q31K73	Uncharacterized protein OS=Synechococcus elongatus (strain PCC 7942) GN=Synpcc7942_2516 PE=4 SV=1	5.12E+07
7	Q31MS5	50S ribosomal protein L34 OS=Synechococcus elongatus (strain PCC 7942) GN=rpmH PE=3 SV=1	2.74E+07
8	P22880	10 kDa chaperonin OS=Synechococcus elongatus (strain PCC 7942) GN=groS PE=3 SV=2	2.59E+07
9	Q31P07	NAD(P)H-quinone oxidoreductase subunit J OS=Synechococcus elongatus (strain PCC 7942) GN=ndhJ PE=3 SV=1	2.37E+07
10	Q935Z3	Trigger factor OS=Synechococcus elongatus (strain PCC 7942) GN=tig PE=3 SV=1	2.17E+07
11	P29801	NAD(P)H-quinone oxidoreductase subunit 2 OS=Synechococcus elongatus (strain PCC 7942) GN=ndhB PE=3 SV=1	2.14E+07
12	Q8KPQ7	Guanylate kinase OS=Synechococcus elongatus (strain PCC 7942) GN=gmk PE=3 SV=2	2.03E+07
13	Q31P08	NAD(P)H-quinone oxidoreductase subunit K OS=Synechococcus elongatus (strain PCC 7942) GN=ndhK PE=3 SV=1	1.82E+07
14	Q31RD2	Ribosome-binding factor A OS=Synechococcus elongatus (strain PCC 7942) GN=rbfA PE=3 SV=1	1.71E+07
15	Q31PT9	Uncharacterized protein OS=Synechococcus elongatus (strain PCC 7942) GN=Synpcc7942_0900 PE=4 SV=1	1.64E+07

16	Q31LP8	Large-conductance mechanosensitive channel OS=Synechococcus elongatus (strain PCC 7942) GN=mscL PE=3 SV=1	1.63E+07
17	Q79PF6	Circadian clock protein KaiA OS=Synechococcus elongatus (strain PCC 7942) GN=kaiA PE=1 SV=1	1.60E+07
18	Q31N52	30S ribosomal protein S4 OS=Synechococcus elongatus (strain PCC 7942) GN=rpsD PE=3 SV=1	1.60E+07
19	Q8GJL5	CBS OS=Synechococcus elongatus (strain PCC 7942) GN=SEM0025 PE=4 SV=1	1.44E+07
20	Q31KS4	ATP synthase subunit beta OS=Synechococcus elongatus (strain PCC 7942) GN=atpD PE=3 SV=1	1.44E+07
21	Q31QF2	60 kDa chaperonin OS=Synechococcus elongatus (strain PCC 7942) GN=groL PE=3 SV=1	1.43E+07
22	P21577	6-phosphogluconate dehydrogenase, decarboxylating OS=Synechococcus elongatus (strain PCC 7942) GN=gnd PE=1 SV=4	1.41E+07
23	Q31MB6	Uncharacterized protein OS=Synechococcus elongatus (strain PCC 7942) GN=Synpcc7942_1773 PE=4 SV=1	1.22E+07
24	P16891	Uroporphyrinogen decarboxylase OS=Synechococcus elongatus (strain PCC 7942) GN=hemE PE=3 SV=2	1.20E+07
25	Q31N54	Uncharacterized protein OS=Synechococcus elongatus (strain PCC 7942) GN=Synpcc7942_1485 PE=4 SV=1	1.15E+07
26	Q31KY2	Uncharacterized protein OS=Synechococcus elongatus (strain PCC 7942) GN=Synpcc7942_2257 PE=4 SV=1	1.00E+07
27	Q31LC1	Uncharacterized protein OS=Synechococcus elongatus (strain PCC 7942) GN=Synpcc7942_2118 PE=4 SV=1	9.78E+06
28	Q31Q75	Uncharacterized protein OS=Synechococcus elongatus (strain PCC 7942) GN=Synpcc7942_0762 PE=4 SV=1	9.75E+06
29	Q31SD0	Uncharacterized protein OS=Synechococcus elongatus (strain PCC 7942) GN=Synpcc7942_0007 PE=4 SV=1	9.58E+06
30	Q31RI3	Uncharacterized protein OS=Synechococcus elongatus (strain PCC 7942) GN=Synpcc7942_0304 PE=4 SV=1	9.40E+06
31	Q31S36	Type 2 NADH dehydrogenase OS=Synechococcus elongatus (strain PCC 7942) GN=Synpcc7942_0101 PE=4 SV=1	9.16E+06
32	Q31NR2	50S ribosomal protein L20 OS=Synechococcus elongatus (strain PCC 7942) GN=rplT PE=3 SV=1	8.69E+06
33	Q31M43	Ribonuclease J OS=Synechococcus elongatus (strain PCC 7942) GN=rnj PE=3 SV=1	8.63E+06
34	Q31LC0	RNA methyltransferase TrmH, group 3 OS=Synechococcus elongatus (strain PCC 7942) GN=Synpcc7942_2119 PE=3 SV=1	7.94E+06
35	Q31S48	Carboxymethylenebutenolidase OS=Synechococcus elongatus (strain PCC 7942) GN=Synpcc7942_0089 PE=4 SV=1	7.53E+06
36	Q31RX9	Rhodanese-like OS=Synechococcus elongatus (strain PCC 7942) GN=Synpcc7942_0158 PE=4 SV=1	7.27E+06
37	Q31L05	NAD(P)H-quinone oxidoreductase subunit N OS=Synechococcus elongatus (strain PCC 7942) GN=ndhN PE=3 SV=1	6.77E+06
38	Q31LY1	Uncharacterized protein OS=Synechococcus elongatus (strain PCC 7942) GN=Synpcc7942_1908 PE=4 SV=1	6.68E+06
39	Q31N63	Uncharacterized protein OS=Synechococcus elongatus (strain PCC 7942) GN=Synpcc7942_1476 PE=4 SV=1	6.66E+06
40	Q31MF5	Ferredoxin-thioredoxin reductase, catalytic chain OS=Synechococcus elongatus (strain PCC 7942) GN=Synpcc7942_1734 PE=3 SV=1	6.60E+06
41	Q31LR4	Uncharacterized protein OS=Synechococcus elongatus (strain PCC 7942) GN=Synpcc7942_1975 PE=4 SV=1	6.58E+06
42	Q31M30	Diguanylate cyclase/phosphodiesterase with PAS/PAC sensor(S) OS=Synechococcus elongatus (strain PCC 7942) GN=Synpcc7942_1859 PE=4 SV=1	5.71E+06
43	Q31RH4	Uncharacterized protein OS=Synechococcus elongatus (strain PCC 7942) GN=Synpcc7942_0313 PE=4 SV=1	5.60E+06
44	Q31MP1	Putative ferric uptake regulator, FUR family OS=Synechococcus elongatus (strain PCC 7942) GN=Synpcc7942_1648 PE=3 SV=1	5.41E+06
45	Q31PV4	Elongation factor G OS=Synechococcus elongatus (strain PCC 7942) GN=fusA PE=3 SV=1	5.40E+06
46	Q31K82	Uncharacterized protein OS=Synechococcus elongatus (strain PCC 7942) GN=Synpcc7942_2507 PE=4 SV=1	5.15E+06
47	Q31Q17	Uncharacterized protein OS=Synechococcus elongatus (strain PCC 7942) GN=Synpcc7942_0820 PE=4 SV=1	5.15E+06
48	P52023	DNA polymerase III subunit beta OS=Synechococcus elongatus (strain PCC 7942) GN=dnaN PE=3 SV=1	4.87E+06
49	O07345	Magnesium-chelatase subunit ChlD OS=Synechococcus elongatus (strain PCC 7942) GN=chlD PE=3 SV=2	4.81E+06
50	Q31MN3	Catalase-peroxidase OS=Synechococcus elongatus (strain PCC 7942) GN=katG PE=1 SV=1	4.49E+06
51	Q31QQ2	PDZ/DHR/GLGF OS=Synechococcus elongatus (strain PCC 7942) GN=Synpcc7942_0585 PE=4 SV=1	4.48E+06
52	Q31NW5	ABC-transporter membrane fusion protein OS=Synechococcus elongatus (strain PCC 7942) GN=Synpcc7942_1224 PE=4 SV=1	4.24E+06
53	Q31K60	Uncharacterized protein OS=Synechococcus elongatus (strain PCC 7942) GN=Synpcc7942_2529 PE=4 SV=1	4.19E+06
54	Q93AK0	Cell division protein Ftn2 OS=Synechococcus elongatus (strain PCC 7942) GN=Synpcc7942_1943 PE=4 SV=1	4.13E+06

55	Q31PH5	CheA signal transduction histidine kinase OS=Synechococcus elongatus (strain PCC 7942) GN=Synpcc7942_1014 PE=4 SV=1	3.92E+06
56	Q31QZ9	Dihydroorotase OS=Synechococcus elongatus (strain PCC 7942) GN=Synpcc7942_0488 PE=3 SV=1	3.85E+06
57	Q31M83	Bacterioferritin comigratory protein OS=Synechococcus elongatus (strain PCC 7942) GN=Synpcc7942_1806 PE=4 SV=1	3.82E+06
58	Q31RA7	Uncharacterized protein OS=Synechococcus elongatus (strain PCC 7942) GN=Synpcc7942_0380 PE=4 SV=1	3.72E+06
59	Q8GAA4	Uncharacterized protein OS=Synechococcus elongatus (strain PCC 7942) GN=sek0026 PE=4 SV=1	3.72E+06
60	Q31S19	Aspartyl/glutamyl-tRNA(Asn/Gln) amidotransferase subunit B OS=Synechococcus elongatus (strain PCC 7942) GN=gatB PE=3 SV=1	3.61E+06
61	Q31RH2	Adenylosuccinate lyase OS=Synechococcus elongatus (strain PCC 7942) GN=Synpcc7942_0315 PE=3 SV=1	3.50E+06
62	Q31LY0	Uncharacterized protein OS=Synechococcus elongatus (strain PCC 7942) GN=Synpcc7942_1909 PE=4 SV=1	3.40E+06
63	Q31NC9	2-isopropylmalate synthase OS=Synechococcus elongatus (strain PCC 7942) GN=leuA PE=3 SV=1	3.38E+06
64	Q31S12	Imidazoleglycerol-phosphate dehydratase OS=Synechococcus elongatus (strain PCC 7942) GN=hisB PE=3 SV=1	3.12E+06
65	P11004	Photosystem II CP43 reaction center protein OS=Synechococcus elongatus (strain PCC 7942) GN=psbC PE=3 SV=3	3.00E+06
66	P50020	Chaperone protein dnaK1 OS=Synechococcus elongatus (strain PCC 7942) GN=dnaK1 PE=3 SV=2	2.99E+06
67	Q31L26	Adenylate kinase OS=Synechococcus elongatus (strain PCC 7942) GN=adk PE=3 SV=1	2.97E+06
68	Q31LQ7	NAD(P)H-quinone oxidoreductase subunit M OS=Synechococcus elongatus (strain PCC 7942) GN=ndhM PE=3 SV=1	2.96E+06
69	P53533	Chaperone protein ClpB 1 OS=Synechococcus elongatus (strain PCC 7942) GN=clpB1 PE=2 SV=3	2.88E+06
70	Q31PH4	Methyl-accepting chemotaxis sensory transducer OS=Synechococcus elongatus (strain PCC 7942) GN=Synpcc7942_1015 PE=4 SV=1	2.85E+06
71	Q31LT9	Uncharacterized protein OS=Synechococcus elongatus (strain PCC 7942) GN=Synpcc7942_1950 PE=4 SV=1	2.73E+06
72	Q31NH5	Uncharacterized protein OS=Synechococcus elongatus (strain PCC 7942) GN=Synpcc7942_1364 PE=4 SV=1	2.70E+06
73	Q31LN3	Uncharacterized protein OS=Synechococcus elongatus (strain PCC 7942) GN=Synpcc7942_2006 PE=4 SV=1	2.64E+06
74	Q31N41	Uncharacterized protein OS=Synechococcus elongatus (strain PCC 7942) GN=Synpcc7942_1498 PE=4 SV=1	2.47E+06
75	Q31M14	Uncharacterized protein OS=Synechococcus elongatus (strain PCC 7942) GN=Synpcc7942_1875 PE=4 SV=1	2.37E+06
76	Q31MF2	Iron-regulated ABC transporter permease protein SufD OS=Synechococcus elongatus (strain PCC 7942) GN=Synpcc7942_1737 PE=4 SV=1	2.25E+06
77	Q935X2	Phospho-2-dehydro-3-deoxyheptonate aldolase OS=Synechococcus elongatus (strain PCC 7942) GN=SEB0024 PE=3 SV=2	2.21E+06
78	Q31QN3	Ribulose-phosphate 3-epimerase OS=Synechococcus elongatus (strain PCC 7942) GN=Synpcc7942_0604 PE=3 SV=1	2.13E+06
79	Q31LU5	Pyruvate dehydrogenase E1 component subunit alpha OS=Synechococcus elongatus (strain PCC 7942) GN=pdhA PE=4 SV=1	1.94E+06
80	Q31S38	Uncharacterized protein OS=Synechococcus elongatus (strain PCC 7942) GN=Synpcc7942_0099 PE=4 SV=1	1.59E+06
81	Q31R39	Zinc metalloprotease OS=Synechococcus elongatus (strain PCC 7942) GN=Synpcc7942_0448 PE=3 SV=1	1.40E+06
82	Q31MS7	Pyridine nucleotide transhydrogenase alpha subunit OS=Synechococcus elongatus (strain PCC 7942) GN=Synpcc7942_1612 PE=4 SV=1	1.29E+06
83	O68523	Response regulator NblR OS=Synechococcus elongatus (strain PCC 7942) GN=nblR PE=4 SV=1	1.22E+06

Supplementary Information Table 4

Model parameters introduced in the modified model. The binding rate constants have units of μm^3 * (molecule^2 * hour)$^{-1}$, and all other rate constants have units of (molecule * hour)$^{-1}$. Rate constants converted to units of (hour)$^{-1}$ and (μM * hour)$^{-1}$ are given in parentheses.

Name	Description	Initial Values	Values used for Figure 4
$\mathrm{kCI_AB_{fs,on}}$	Rate of fsKaiB binding to active KaiC hexamers	5.4×10^2 (3.3×10^5)	1.4×10^2 (8.6×10^4)
$\mathrm{kCI_AB_{gs,on}}$	Rate of ground state KaiB binding to active KaiC hexamers	1.7×10^{-4} (1.0×10^{-1})	4.5×10^{-5} (2.8×10^{-2})
$\mathrm{kCI_AB_{fs,off}}$	Rate of KaiB unbinding from active KaiC hexamers as fsKaiB	3.7 (3.7)	1.3×10^2 (1.3×10^2)
$\mathrm{kCI_IB_{fs,on}}$	Rate of fsKaiB binding to inactive KaiC hexamers	4.0×10^3 (2.4×10^6)	2.4×10^3 (1.5×10^6)
$\mathrm{kCI_IB_{gs,on}}$	Rate of ground state KaiB binding to inactive KaiC hexamers	1.4×10^{-1} (84)	3.8×10^{-1} (2.2×10^2)
$\mathrm{kCI_IB_{fs,off}}$	Rate of KaiB unbinding from inactive KaiC hexamers as fsKaiB	9.2×10^{-3} (9.2×10^{-3})	5.0×10^{-1} (5.0×10^{-1})
$\mathrm{kBswitch_f}$	Rate of KaiB activation (fold switching)	1.9×10^{-1} (1.9×10^{-1})	1.7×10^{-2} (1.7×10^{-2})
$\mathrm{kBswitch_r}$	Rate of KaiB inactivation (reversion to ground state)	2.2×10^3 (2.2×10^3)	4.3×10^1 (4.3×10^1)
$\mathrm{kKidA_{on}}$	Rate of KidA binding to fsKaiB	22 (1.3×10^4)	1.2×10^2 (7.2×10^4)
$\mathrm{kKidA_{off}}$	Rate of KidA unbinding from KaiB	7.8 (7.8)	1.1×10^1 (1.1×10^1)

Supplementary References

1. S. S. Golden, J. Brusslan, R. Haselkorn, Expression of a family of psbA genes encoding a photosystem II polypeptide in the cyanobacterium Anacystis nidulans R2. *The EMBO Journal* **5**, 2789-2798 (1986).
2. S. R. Mackey, J. L. Ditty, E. M. Clerico, S. S. Golden, Detection of rhythmic bioluminescence from luciferase reporters in cyanobacteria. *Methods Mol Biol* **362**, 115-129 (2007).
3. G. K. Pattanayak, G. Lambert, K. Bernat, M. J. Rust, Controlling the Cyanobacterial Clock by Synthetically Rewiring Metabolism. *Cell Rep* **13**, 2362-2367 (2015).
4. L. Kall, J. D. Storey, W. S. Noble, Non-parametric estimation of posterior error probabilities associated with peptides identified by tandem mass spectrometry. *Bioinformatics* **24**, i42-i48 (2008).
5. E. Leypunskiy *et al.*, The cyanobacterial circadian clock follows midday in vivo and in vitro. *Elife* **6** (2017).
6. L. A. Kelley, S. Mezulis, C. M. Yates, M. N. Wass, M. J. Sternberg, The Phyre2 web portal for protein modeling, prediction and analysis. *Nat Protoc* **10**, 845-858 (2015).
7. W. Humphrey, A. Dalke, K. Schulten, VMD: visual molecular dynamics. *J Mol Graph* **14**, 33-38, 27-38 (1996).
8. J. Paijmans, D. K. Lubensky, P. R. Ten Wolde, A thermodynamically consistent model of the post-translational Kai circadian clock. *PLoS Comput Biol* **13**, e1005415 (2017).
9. J. Goodman, J. Weare, Ensemble samplers with affine invariance. *Communications in Applied Mathematics and Computational Science* **5**, 65-80 (2010).
10. F. Madeira *et al.*, The EMBL-EBI search and sequence analysis tools APIs in 2019. *Nucleic Acids Res* **47**, W636-W641 (2019).
11. U. Römling, M. Y. Galperin, M. Gomelsky, Cyclic di-GMP: the First 25 Years of a Universal Bacterial Second Messenger. *Microbiology and Molecular Biology Reviews* **77**, 1-52 (2013).
12. J. T. Henry, S. Crosson, Ligand-binding PAS domains in a genomic, cellular, and structural context. *Annu Rev Microbiol* **65**, 261-286 (2011).